AD 442524

442524

Technical Report...

STUDY OF PULSED RADIATION EFFECTS ON MICROWAVE FERRITE DUPLEXERS

SEVENTH QUARTERLY REPORT

1 November 1963 to 29 February 1964

Report No. 7 Contract No. DA-36-039-SC-89113

DEPARTMENT OF THE ARMY TASK NUMBER
OST 5974 01 004 36 00

This research on Transient Radiation Effects on Electronics is sponsored by the Defense Atomic Support Agency, and is conducted under the technical guidance of the U. S. Army Electronics Research and Development Laboratories, Ft. Monmouth, New Jersey, 07703, and the DASA-TREE Program Manager.

U. S. ARMY ELECTRONICS RESEARCH
AND DEVELOPMENT LABORATORIES
FORT MONMOUTH, NEW JERSEY

SPERRY
MICROWAVE ELECTRONICS COMPANY
CLEARWATER FLORIDA

SEVENTH QUARTERLY REPORT

STUDY OF PULSED RADIATION EFFECTS ON MICROWAVE FERRITE DUPLEXERS

1 November 1963 to 29 February 1964

Report No. 7

Contract No. DA 36-039-SC-89113

DEPARTMENT OF THE ARMY TASK NUMBER
OST 5974 01 004 36 00

March 1964

Study effects of pulsed nuclear radiation on the operating characteristics of C-Band microwave coaxial ferrite Y-junction circulators and gyromagnetic coupling limiters.

This research on Transient Radiation Effects on Electronics is sponsored by the Defense Atomic Support Agency, and is conducted under the technical guidance of the U. S. Army Electronics Research and Development Laboratories, Ft. Monmouth, New Jersey. 07703, and the DASA-TREE Program Manager.

Prepared by:

R. E. Greenwood
G. R. Harrison

Approved by:

Dr. E. W. Matthews

SPERRY MICROWAVE ELECTRONICS COMPANY
DIVISION OF SPERRY RAND CORPORATION
CLEARWATER, FLORIDA

SJ-222-0041-7

Copy No. 150

TABLE OF CONTENTS

LIST OF ILLUSTRATIONS

LIST OF ILLUSTRATIONS (CONT.)

LIST OF TABLES

1. PURPOSE

The general purpose of the second year of this study is to extend the study of pulsed nuclear radiation effects on the operating characteristics of coaxial C-band beacon ferrite duplexer devices and to include the study of pulsed nuclear radiation effects on the operating characteristics of waveguide ferrite duplexing devices operating under both high and low r-f power conditions. The coaxial duplexer to be investigated further was developed by the Sperry Microwave Electronics Company under Contract No. DA36-039-SC-85330. The four-port, differential phaseshift, waveguide duplexer and the Y-junction waveguide circulator to be investigated were also developed by the Sperry Microwave Electronics Company for use in various types of radar and communication applications. Experimental radiation effects data are to be acquired for the duplexers and/or their components operating in a frequency range of 5.4 to 5.9 Gc and at least two r-f power levels, one below one watt (low power) and the other as high as possible (expected to be near 5 kilowatts peak).

Specifically, the aims of the seventh quarter of the study were the following:

- To perform a fifth series of experiments at the Sandia Pulsed Reactor Facility (SPRF), during the week of 2 December 1963, involving irradiation of the individual waveguide and coaxial duplexer components and assembled coaxial duplexer. The components were operated under two levels of power approximately equal to 100 milliwatts cw and 5 kilowatts pulsed.
- To reduce and analyze the data recorded during the fifth series of experiments.

2. ABSTRACT

This report presents the results of the fifth series of radiation environmental experiments conducted during the seventh quarter of the program. Included in the report are a description of the equipment used to perform the experiments, the measurement techniques employed, and a complete dosimetry report. Photographs of important phases of the test are given to provide the reader with a better insight into the study. The microwave high power tests, which were initiated during the fourth series of tests, were continued for the fifth series of experiments. Conclusions presented are based upon the data taken thus far, including the fourth and fifth series of tests with high power operation.

3. PUBLICATIONS, LECTURES, REPORTS AND CONFERENCES

3.1 PUBLICATIONS

No additional publications were generated during this reporting period.

3.2 LECTURES

None in this reporting period.

3.3 REPORTS

None in this reporting period.

3.4 CONFERENCES

A conference was held on 17 December 1963, at the U. S. Army Electronics Research and Development Laboratory, Fort Monmouth, New Jersey. In attendance from the U. S. Army Electronics Research and Development Laboratory were:

L. L. Kaplan
F. Palmisano
William H. Wright
John Carter

In attendance from Sperry was: G. R. Harrison.

The purpose of this conference was to analyze and review the results of the program to date and to discuss and formalize the scope and plans to be followed for the remainder of the program.

4. FACTUAL DATA

4.1 EXPERIMENTAL PROCEDURES

4.1.1 Introduction

The fifth series of tests was conducted to extend the information obtained on the coaxial and waveguide components tested previously[1,2,3,4,5,6] and to continue a study of these components operating under a much higher power level than earlier experiments. Low power microwave experiments are conducted using approximately 100 milliwatts of cw power to drive the components under test. High power microwave tests employ a magnetron power source to drive the components under test with approximately 5 kilowatts of peak power. The high power source delivers two r-f pulses approximately 10 microseconds in width with a separation of 150 microseconds. The first pulse, hereafter called P1, was delayed from the control room (SPRF) synchronization trigger by approximately 220 microseconds. This delay placed P1 under the radiation burst. The second burst of rf, hereafter called P2, could be delayed up to 150 microseconds following P1. The delay was normally set for the maximum of 150 microseconds. The two-pulse system was desirable because it provided a means to observe the effects during the radiation burst as well as any lingering effects following the burst.

Three low power sources were employed to perform backup experiments to the high power tests and to extend the data taken on previous trips to the reactor. Only one experiment at high r-f power was performed during each radiation burst. Both the low and high power sources were operated at a frequency of 5.6 Gc. Block diagrams of the high and low power sources utilized during the fifth series of experiments are the same as shown in the previous report.[6]

The signal produced by the power source, designated monitor signal, was observed during each burst to insure that no changes occurred in the driving power. This was accomplished by using a directional coupler to sample the power delivered by the source which was detected and monitored on a scope. Also, the power reflected from the component under test, designated VSWR signal, was monitored by using a circulator (low power) or a directional coupler (high power) between the source and the component under test.

On the two-port devices tested, such as limiters, waveguides, and isolators, the return signal from the device was monitored. When three-port devices (circulators, duplexers, etc.) were tested, the power was delivered to the transmitter port, and the return signals from the antenna and receiver were monitored.

The following parts of this section (4.1) present a description of the procedure and the components tested during the fifth series of tests. Section 4.2 contains an analysis of the results obtained during the experiments.

4.1.2 Waveguide-to-Coaxial Adapter Tests

Previous data have indicated some discrepancies in the results when waveguide-to-coaxial adapters were used at the test component. All input and output transmission lines were coaxial cable. When waveguide sections and waveguide components were tested, adapters were required to test these components. Nine separate adapters have been used in previous experiments. Some of these adapters contained polyethylene matching beads and others used Rexolite beads. Previous data indicated that the match into the adapters was affected by the nuclear radiation. Some experiments were performed therefore during the fifth series of experiments to evaluate these adapters using the different bead types to the extent that any effects observed could be noted and taken into account when evaluating and testing waveguide components. Tests were performed at both high and low power.

Figure 1 shows a typical return signal at low power from a set of adapters with polyethylene beads.

Figure 2 is a photograph of the test setup at the SPRF.

4.1.3 Waveguide Tests

Sections of C-band aluminum waveguide (air filled and high density polyfoam filled) were tested while operating under low power conditions. Figure 3 shows the waveguide section in test positions in the SPRF. Figure 4 presents a typical photograph of the reaction which occurred in a one-foot section of air filled aluminum C-band waveguide operating under approximately 100 milliwatts cw.

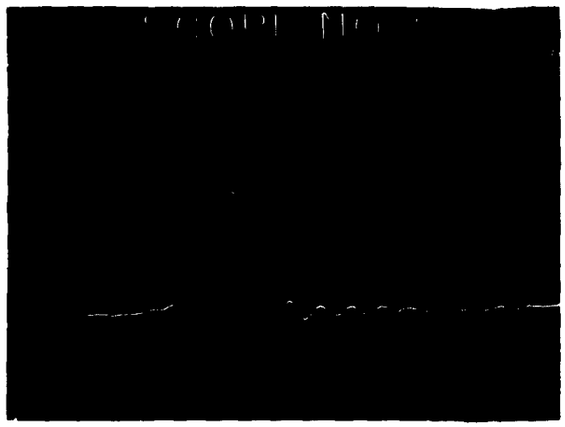

Return Signal
Vertical Sensitivity 0.005 volts/cm
Horizontal Sweep Speed 50 μsec/cm

Figure 1. Burst No. 4, waveform of the return signal from a set of waveguide-to-coaxial adapters(polyethylene beads) operating under low r-f power at 5.6 Gc.

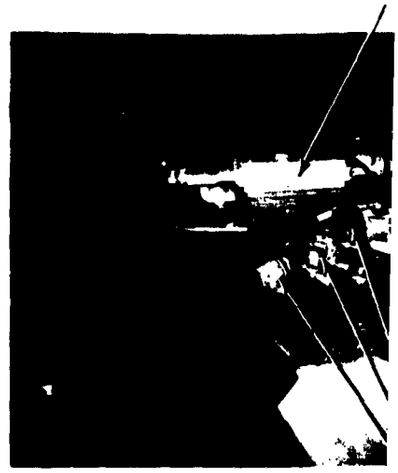

WAVEGUIDE-
ADAPTE

Figure 2. Typical test configurati raising the reactor into The components clockw reactor hole were a wa and three separate set- to-coaxial adapters.

Figure 3. Reactor scene showing a waveguide duplexer (upper left), an aluminum waveguide test section (just under waveguide duplexer), a waveguide Y- junction circulator, and a coaxial duplexer in test position.

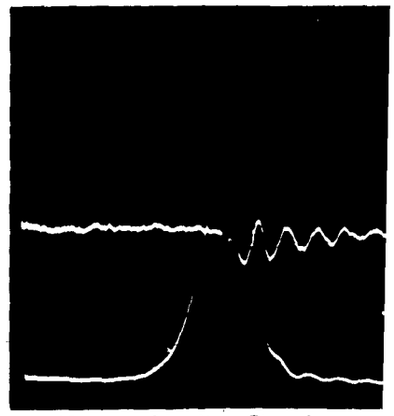

Upper Trace: Monitor Signal
Vertical Sensitivity
Horizontal Sweep Sp

Lower Trace: Return Signal
Vertical Sensitivity
Horizontal Sweep Sp

Figure 4. Input and output signa of aluminum C-band ating at 100 milliwatt

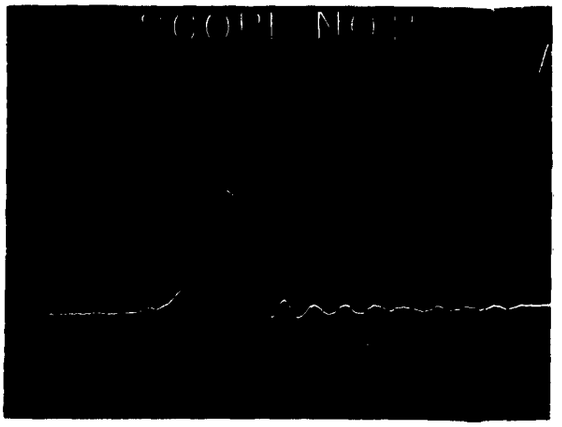

Return Signal
Vertical Sensitivity 0.005 volts/cm
Horizontal Sweep Speed 50 μsec/cm

Figure 1. Burst No. 4, waveform of the return signal from a set of waveguide-to-coaxial adapters(polyethylene beads) operating under low r-f power at 5.6 Gc.

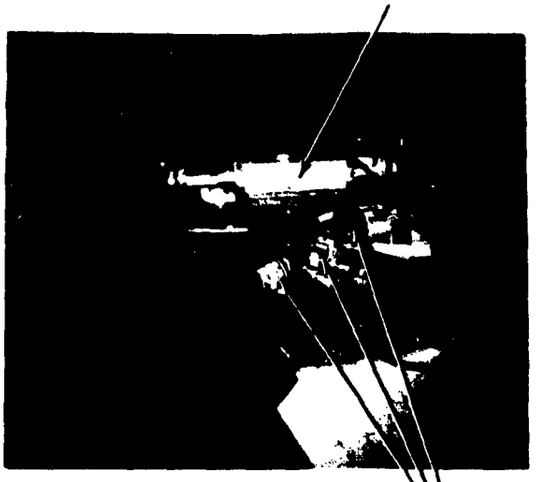

Figure 2. Typical test configuration seen before raising the reactor into test position. The components clockwise around the reactor hole were a waveguide duplexer and three separate set-ups of waveguide-to-coaxial adapters.

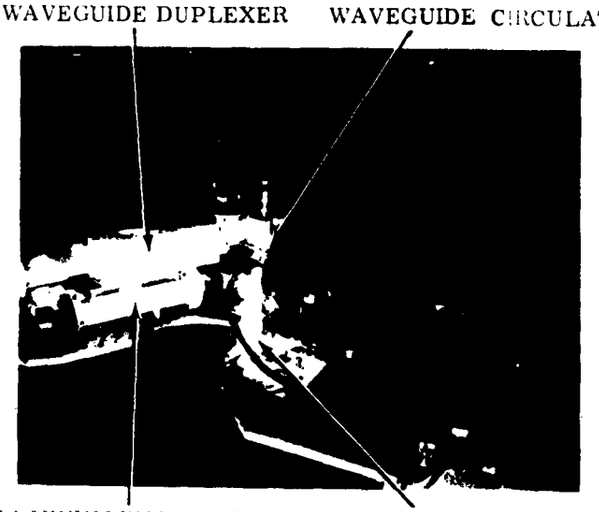

Figure 3. Reactor scene showing a waveguide duplexer (upper left), an aluminum waveguide test section (just under waveguide duplexer), a waveguide Y-junction circulator, and a coaxial duplexer in test position.

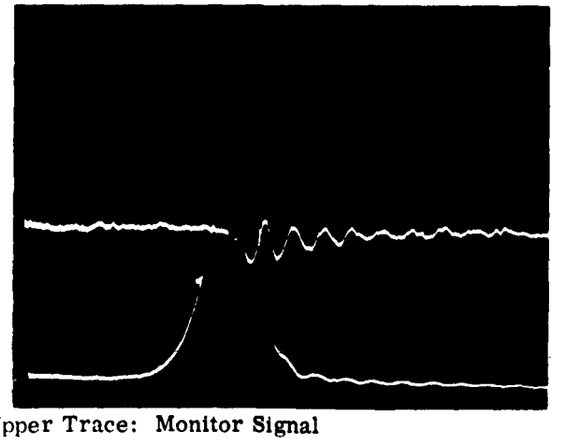

Upper Trace: **Monitor Signal**
Vertical Sensitivity 0.005 volts/cm
Horizontal Sweep Speed 50 μsec/cm
Lower Trace: Return Signal
Vertical Sensitivity 0.005 volts/cm
Horizontal Sweep Speed 50 μsec/cm

Figure 4. Input and output signals on a section of aluminum C-band waveguide operating at 100 milliwatts cw at 5.6 Gc.

4.1.4 Coaxial Isolator

A C band, internal magnet, coaxial isolator was tested in the reactor operating under low power. The isolator was driven in the forward direction, i.e., the direction of low insertion loss. A typical return signal is shown in Figure 5.

4.1.5 Coaxial Circulator

A C-band ferrite, Y-junction, coaxial circulator was tested while operating under high power. The antenna port was monitored for changes in the insertion loss. Figure 6 presents the typical test data of the reaction observed on the antenna port of a coaxial circulator operating at high power.

4.1.6 Coaxial Limiter

A relatively small reaction has been observed on a gyromagnetic coaxial limiter in past experiments when operating the component under low power. However, in these tests the limiter was operating at power levels below the limiting threshold. During the fourth and fifth series of tests, the coaxial limiter was driven with the high power source. During the fourth series of experiments it was observed that signal through the limiter increased by approximately 10 db. This was interpreted as a 10 db transient increase in the limiting threshold of the limiter.

During the fifth set of experiments the limiter was again evaluated at low and high r-f power. Figure 7 depicts the typical test data of the limiter at low power (100 milliwatts) during Burst 12. Similar data were obtained during Burst 13. High power tests were performed on the same limiter during Burst 14. With an oscilloscope vertical sensitivity of 0.02 volts/cm, the reaction went off scale. The data shown in Figure 8 were obtained during Burst 15 with a vertical sensitivity of 2 volts/cm. For data comparison the calibration data are shown in Figure 9. The same limiter was under test during Burst 16, but no acceptable data were obtained. No signal was observed from the limiter in Burst 16. Calibration photographs before burst time were acceptable. For Burst 17 a new limiter was tested. Time did not permit calibration before the radiation burst. The data obtained indicated an increase of the signal through the limiter during the burst. No signals could be obtained from the limiter for calibration after the burst.

During Burst 18 the original (first) limiter was tested at low power. The data obtained are depicted in Figure 10.

The test configuration of the limiter is shown in Figure 11.

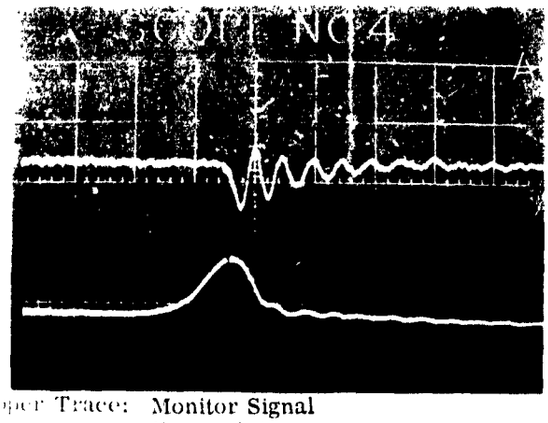

Upper Trace: Monitor Signal
Vertical Sensitivity 0.005 volts/cm
Horizontal Sweep Speed 50 μsec/cm

Lower Trace: Return Signal
Vertical Sensitivity 0.005 volts/cm
Horizontal Sweep Speed 50 μsec/cm

Figure 5. Burst No. 6, monitor and return signal (insertion loss) from a coaxial isolator operating at low power, cw, at 5.6 Gc.

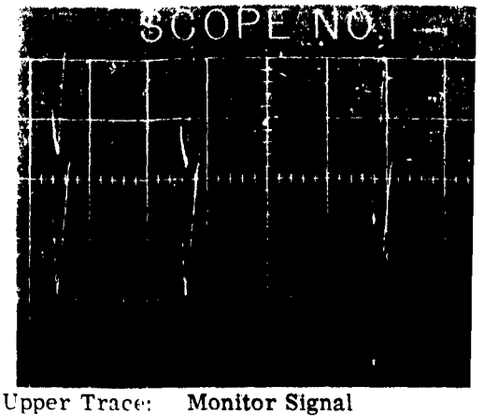

Upper Trace: Monitor Signal
Vertical Sensitivity 0.1
Horizontal Sweep 50 μsec

Lower Trace: Antenna Return
Vertical Sensitivity 0.005
Horizontal Sweep 50 μsec

Figure 6. Burst 18, test data obtained the monitor and antenna ret C-band coaxial Y-junction operating at high power at 5

NOTE: The first and third pulse groups from and P2, respectively, before burst. fourth pulse groups are P1 and P2 dur

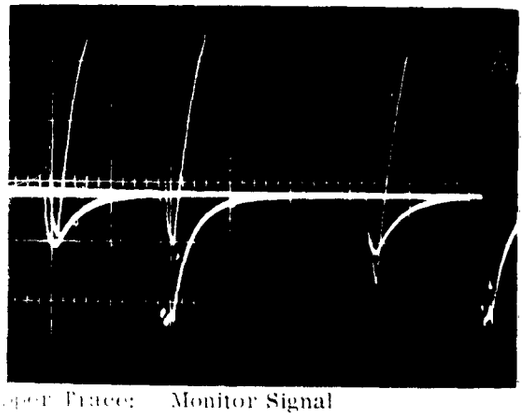

Upper Trace: Monitor Signal
Vertical Sensitivity 0.2 volts/cm

Lower Trace: Return Signal
Vertical Sensitivity 2 volts/cm

Figure 8. Burst No. 16, waveforms of input and output signals from gyromagnetic coupling coaxial limiter operating under high power at 5.6 Gc.

First and third pulse groups from the left are P1 and P2, respectively, before burst. The second and fourth pulse groups are P1 and P2 during burst time

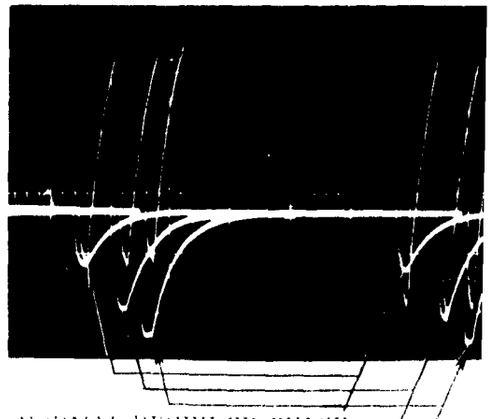

Lower Trace: Return Signal Calibrate
Vertical Sensitivity 2
Horizontal Sweep 50 μsec

Figure 9. Burst 15, calibration data for the return signal from the magnetic coupling limiter at 5.6 Gc.

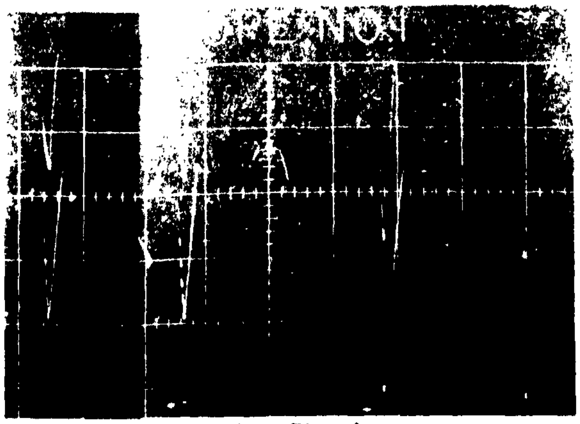

Upper Trace Monitor Signal
Vertical Sensitivity 0.1 volts/cm
Horizontal Sweep 50 μsec/cm

Lower Trac Antenna Return
Vertical Sensitivity 0.005 volts/cm
Horizontal Sweep 50 μsec/cm

Figure 6. ... t 15, test data obtained from ... monitor and antenna return of a ... and coaxial Y-junction circulator ... ating at high power at 5.6 Gc.

NOTE: The first ... third pulse groups from the left are P1 and P2, ... ectively, before burst. The second and fourth pu... groups are P1 and P2 during burst time.

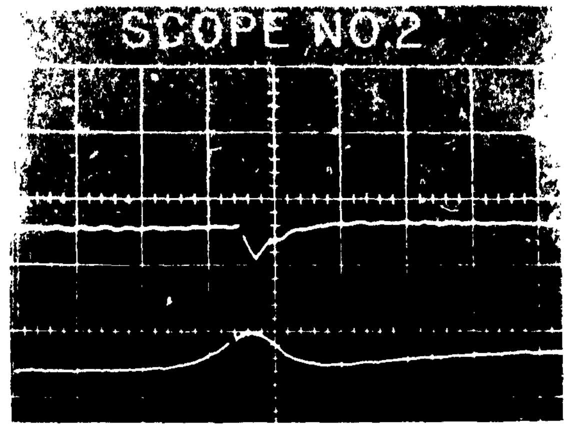

Upper Trace: Monitor Signal
Vertical Sensitivity 0.005 volts/cm

Lower Trace: Return Signal
Vertical Sensitivity 0.005 volts/cm
Horizontal Sweep 50 μsec/cm

Figure 7. Burst 12, monitor and return signals from the gyromagnetic coupling coaxial limiter operating at low power at 5.6 Gc.

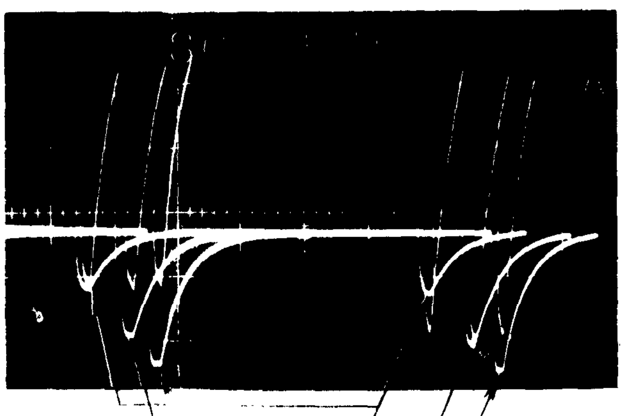

... ED PULSE
... DB ... ASE IN SIGNAL
... DB ... EASE IN SIGNAL

Lower Trac ... Signal Calibration
... rtical Sensitivity 2 volts/cm
... zontal Sweep 50 μsec/cm

Figure 9. ... calibration data (high power) ... turn signal from the gyro- ... coupling limiter operating at

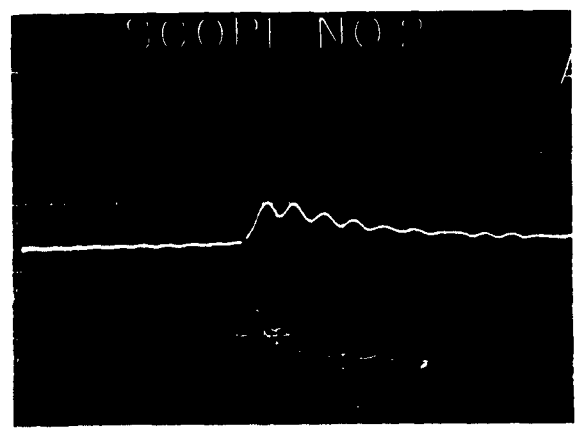

Upper Trace: Monitor Signal
Vertical Sensitivity 0.005 volts/cm

Lower Trace: Return Signal
Vertical Sensitivity 0.005 volts/cm
Horizontal Sweep 50 μsec/cm

Figure 10. Burst 18, monitor and return signals from gyromagnetic coupling coaxial limiter operating at low power at 5.6 Gc.

2

[illegible] Coaxial Diplexer [illegible]

A C-band coaxial ferrite diplexer [illegible] tested [illegible] operating [illegible] high and low power. The antenna and receiver ports [illegible] for changes in the insertion loss and isolation, respectively. Figure [illegible] presents [illegible] on the antenna and receiver ports of a C-band coaxial ferrite diplexer operating under low power cw at [illegible] GHz. Figure 13 depicts the input and output signals from the antenna port of the coaxial diplexer under high-power operation. Figure [illegible] shows [illegible] coaxial diplexer in test position at the SPRI.

[illegible] 8 Waveguide Junction Circulator

The C-band Y-junction waveguide circulator was tested operating under both high and low power. The antenna and receiver ports were monitored for changes in insertion loss and isolation, respectively, during the radiation burst. Figure 14 presents the input and return signals from the antenna (also the VSWR signal). These return signals indicate an increase in insertion loss between the transmitter and antenna ports of the device and a decrease in isolation between the transmitter and receiver ports. Figure [illegible] presents the return signal from the antenna port of the circulator operating at 5.[illegible] GHz and high pulsed rf power. Figure [illegible] shows a waveguide circulator in test position in the SPRI.

[illegible] 9 Waveguide Differential-Phase-Shift Duplexer

A waveguide, phase shift, ferrite duplexer was exposed to the radiation burst while operating under both high pulsed power and low cw power. As with the [illegible] of [illegible], the antenna and receiver ports were monitored during the burst. Figure [illegible] presents the return signals from the antenna and receiver ports of a waveguide duplexer operating under [illegible] power at [illegible] GHz. Figure [illegible] presents the return signal from the antenna port of [illegible] duplexer operating under high pulsed power [illegible]. Figure [illegible] shows [illegible] in test position at the SPRI.

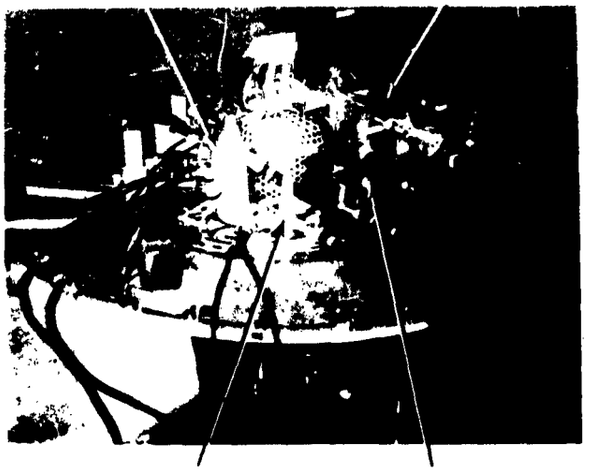

COAXIAL LIMITER WAVEGUIDE CIRCULATOR

Figure 11. Test configuration at the SPRF. The components are as follows (clockwise, starting with component in upper right hand corner): waveguide duplexer, waveguide circulator, coaxial limiter, and coaxial duplexer.

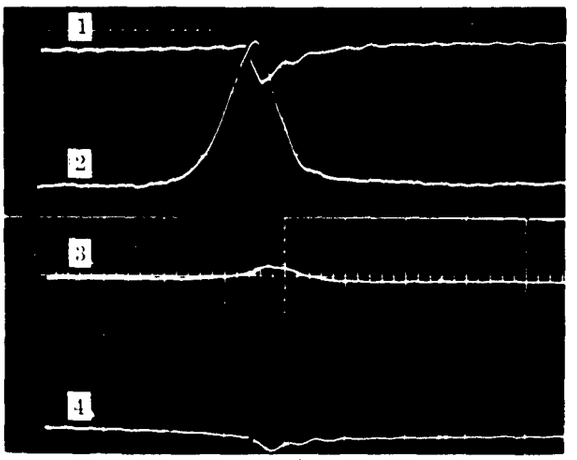

Trace 1: Monitor Signal
Vertical Sensitivity 0.005 volts/cm
Trace 2: Return Signal (Antenna Port)
Vertical Sensitivity 0.005 volts/cm
Trace 3: VSWR Signal
Vertical Sensitivity 0.01 volts/cm
Trace 4: Return signal (Receiver Port)
Vertical Sensitivity 0.005 volts/cm

Figure 14. Burst No. 9, waveform of the input VSWR, and the output signal from the antenna and receiver ports of a C-band, Y-junction, waveguide circulator operating under cw low power

Upper Trace: Monitor Signal
Vertical Sensitivity
Middle Trace: Return Signal (Ante
Vertical Sensitivity
Lower Trace: Receiver Return Sig
Vertical Sensitivity
Horizontal Sweep Sp

Figure 12. Burst No. 6, waveform
signal from the antenna
ports of a C-band coaxi
plexer operating unde
wer at 5.6 Gc.

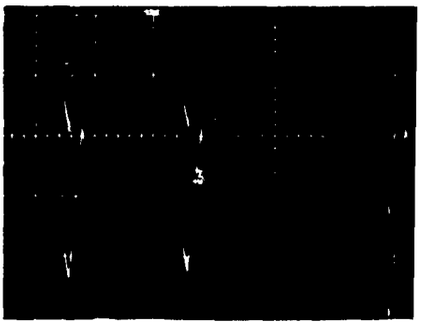

Upper Trace: Monitor Signal
Vertical Sensitivi

Lower Trace: Antenna Return Sign
Vertical Sensitivity
Horizontal Sweep S

Figure 15. Burst No. 12, waveform
and return signal from t
port of a C-band Y-junct
guide circulator oper
pulsed low power

1

Upper Trace: Monitor Signal
rtical Sensitivity 0.005 volts/cm
Middle Trace: turn Signal (Antenna Port)
rtical Sensitivity 0.005 volts/cm
Lower Trace: ceiver Return Signal
rtical Sensitivity 0.005 volts/cm
rizontal Sweep Speed 50 μsec/cm

Figure 12. No. 6, waveform of the output from the antenna and receiver ports of a C-band coaxial ferrite operating under cw low power at 5.6 Gc.

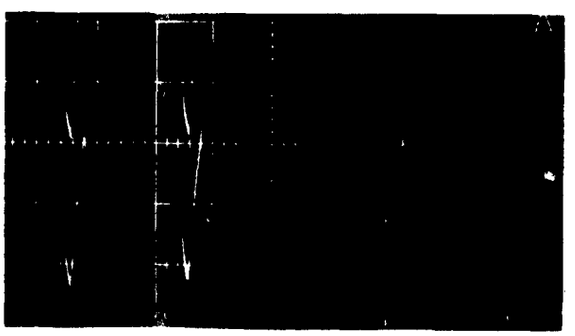

Upper Trace: tor Signal
cal Sensitivity 0.1 volts/cm
Lower Trace: Return Signal
cal Sensitivity 0.05 volts/cm
zontal Sweep Speed 50 μsec/cm

Figure 14. 12, waveform of monitor signal from the antenna C-band Y-junction wave- ator operating under high power at 5.6 Gc.

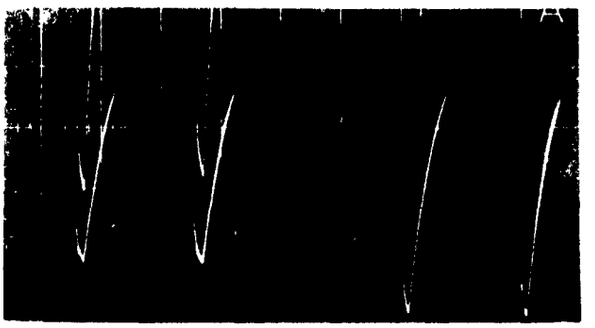

Upper Trace: Monitor Signal
Vertical Sensitivity 0.1 volts/cm
Lower Trace: Return Signal
Vertical Sensitivity 0.1 volts/cm
Horizontal Sweep 50 μsec/cm

Figure 13. Burst No. 9, waveforms of the input and the output signal from the antenna port of a C-band coaxial ferrite duplexer operating under high pulsed power at 5.6 Gc.

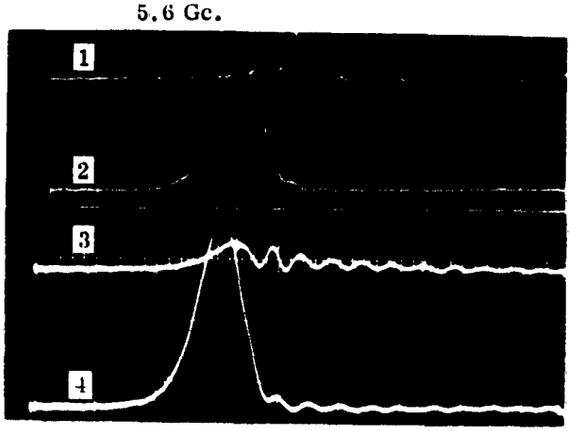

Trace 1: Monitor Signal
Vertical Sensitivity 0.005 volts/cm

Trace 2: Return Signal (Antenna Port)
Vertical Sensitivity 0.01 volts/cm

Trace 3: VSWR Signal
Vertical Sensitivity 0.005 volts/cm

Trace 4: Return Signal (Receiver Port)
Vertical Sensitivity 0.01 volts/cm
Horizontal Sweep 50 μsec/cm

Figure 16. Burst No. 3, waveform from monitor VSWR, and output signals of the antenna and receiver ports of a waveguide, phase shift, ferrite duplexer operating under low cw power at 5.6 Gc.

4.1.10 Additional Components

The MA-220 magnetron tube alone with no associated circuitry was placed adjacent to the reactor during the last two bursts. The magnetron was single pulsed such that the pulse was coincident with the radiation burst. The power output was monitored preburst and during the burst. No changes in the output level were observed. In the fourth series of tests,[6] a large decrease in output power was observed when this same magnetron was tested along with the pulse transformer and its associated circuitry. This decrease in output power is due to the transient effects in the transformer and associated circuitry rather than the magnetron itself, as verified by the data obtained on the above tests (fifth series of tests). The magnetron is shown in test position at the SPRF in Figure 18.

A C-band coaxial frequency meter (transmission cavity type) was tested during the fifth series of experiments. No calibration data were obtainable but a large excursion is noted in the output signal. This indicates that the resonance characteristics of the cavity were altered during the radiation burst. The ionized air possibly produced a phase change in the r-f signal as it traversed the sharply tuned cavity.

4.2 ANALYSIS OF DATA AND RESULTS

4.2.1 Calibration Procedures

The millivolt deflections observed on the oscilloscopes were converted to db changes in the operating characteristics of the components by use of calibrated variable attenuators placed between the r-f sources and the component under test. Before burst time, attenuations of 0, 0.5, 1.0, 2.0, and 3.0 db were introduced into the transmission lines, and photographs were taken of the output level of each crystal detector. From these photographs the change in attenuation in db was plotted as a function of the change in the voltage output level in millivolts of each crystal. Because these curves were very close to being linear in most cases, the crystal sensitivities were approximately constant and had dimensions of millivolts/db. This constant crystal sensitivity is recorded in the following tables which present the results of the tests.

Since large increases were observed in the return signal from the power limiter, fixed attenuators were removed from the signal return line for calibration of the magnitude of the increase. Typical calibration data are shown in Figure 9.

The following sections present the results obtained on the transient radiation effects in the components and the conclusions reached from these effects.

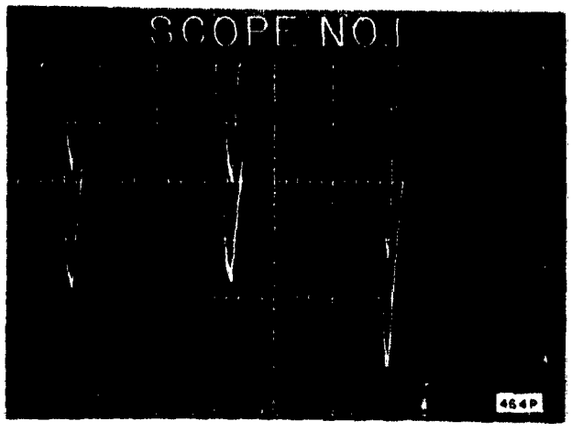

Upper Trace: Monitor Signal
Vertical Sensitivity 0.1 volts/cm

Lower Trace: Return Signal (Antenna)
Vertical Sensitivity 0.1 volts/cm
Horizontal Sweep 50 μsec/cm

Figure 17. Burst No. 5, waveform of the monitor and output signal from the antenna port of a waveguide, phase shift, ferrite duplexer operating under high pulsed power at 5.6 Gc.

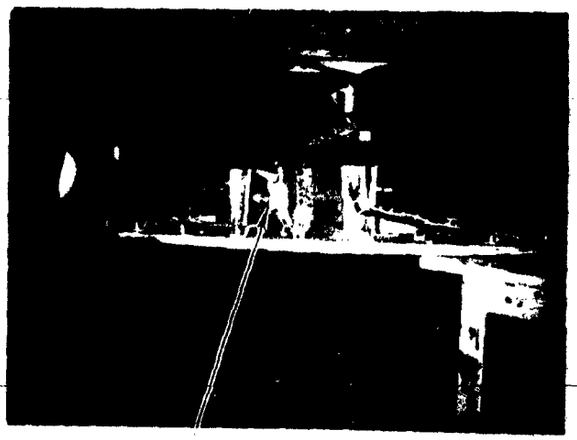

MAGNETRON MX-220

Figure 18. The MX-220 magnetron in test position at the SPRF.

4.2.2 Transient Radiation Effects in the Components Tested

Waveguide to Coaxial Adapters. The effects observed during the waveguide-to-coaxial adapter tests are presented in Table I. For the high power tests, the effects observed for the first pulse, P1, are tabulated separately from those of the second pulse, P2. Polarities indicate whether the changes were increases or decreases in isolation or insertion loss. A positive sign indicates the signal being monitored increased, and a negative sign indicates the signal decreased. Any changes in the high power signals levels less than 0.1 db are considered insignificant due to the error associated with calibration.

The following explanations are for Tables I through V:

- Column 1 of Table I assigns an identification number to each reaction for reference purposes.
- Column 2 is the burst number assigned by Sperry, i.e., the first burst during the tests was assigned number 1.
- Column 3 gives the change in temperature of the reactor for each burst as supplied by the SPRF personnel.
- Column 4 is the oscilloscope channel number which recorded the reaction.
- Column 5 gives the name of the component being tested.
- Column 6 lists the power source driving the component.
- Column 7 gives the crystal detector number used to monitor the signal concerned.
- Column 8 presents the crystal sensitivity as calculated from the calibration curves.
- Column 9 gives the sensitivity of the oscilloscope channel monitoring the signal.
- Column 10 presents the magnitude of the deflection observed on the oscilloscope.
- Column 11 lists the effect in db as calcutated from columns 8 and 10.
- Column 12 lists the signal monitored.

Four sets of adapters (labeled #1, #2, #3, #4) were tested at low and high power. Rexolite and polyethylene matching beads were evaluated in each adapter.

The following conclusions are offered regarding the waveguide-to-coaxial adapters from the data in Table I:

- The average transient decrease in signal level passing through the adapters using Rexolite beads was approximately 0.1 db while operating in the 100 milliwatt level at 5.6 Gc.

TABLE I. RESULTS OF RADIATION E
TO COAXIAL ADAP
HIGH AND LOW

1	2	3	4	5
IDENTIFICATION NO.	BURST NO.	BURST NO.	INPUT NO.	COMPONENT UNDER TEST
1	1	96.5	1	WAVEGUIDE TO COAXIAL ADAPTER #1 (REXOLITE BEAD)
2	1	96.5	2	#1
3	1	96.5	4	#3
4	1	96.5	8	#4
5	1	96.5	11	#3
6	2	96.0	1	#1
7	2	96.0	2	#1
8	2	96.0	4	#3
9	2	96.0	8	#4
10	3	105.5	2	WAVEGUIDE TO COAXIAL ADAPTER #1 (POLYETHYLENE BEAD
11	3	105.5	4	#3
12	3	105.5	8	#4
13	3	105.5	11	#3
14	4	106.2	2	#1
15	4	106.2	4	#3
16	4	106.2	8	#4
17	4	106.2	11	#3

NOTES: 1. WHERE THERE ARE TWO VALUES GIVEN, THE FIRST CORRESPONDS TO THE HIGH POWER PULSE (P1) DELAYED ~200 μSECONDS AFTER THE SPR TRIGGER; AND THE SECOND VALUE CORRESPONDS TO THE PULSE (P2) ~ 350 μSECONDS AFTER THE SPR TRIGGER.

2. POSITIVE SIGNS INDICATE AN INCREASE IN POWER AT THE POINT OF MEASUREMENT.

3. MONITOR: DETECTOR MONITORING THE INPUT SIGNAL LEVEL.
VSWR: DETECTOR MONITORING THE VSWR OF THE DEVICE.
RETURN: DETECTOR MONITORING THE RETURN SIGNAL FROM THE DEVICE.

4. LOW CW - APPROXIMATELY 100 MILLIWATTS CW AT THE COMPONENT UNDER TEST.
HIGH PULSED - APPROXIMATELY 5KW PEAK AT THE COMPONENT UNDER TEST.

TABLE I. RESULTS OF RADIATION ENVIRONMENT TESTING OF WAVEGUIDE TO COAXIAL ADAPTERS AT 5.6 GC FOR R-F HIGH AND LOW POWER CONDITIONS

5	6		7	8	9	10	11	12
PONENT UNDER TEST	DRIVING	SIGNAL[4]	CRYSTAL DETECTOR NO.	CRYSTAL SENSITIVITY (MV/DB)[1]	VERTICAL GAIN (MV CM)	MAGNITUDE OF EFFECT (MV)[1, 2]	MAGNITUDE OF EFFECT (DB)[1, 2]	SIGNAL[3]
L ADAPTER #1 (REXOLITE BEAD)	HIGH	PULSED	1	224	100	-8, -6	-. 04, -. 03	MONITOR
#1	HIGH	PULSED	1	148, 144	100	+6, +6	+. 04, +. 04	RETURN
#3	LOW	CW	13	90	5	-8	-. 09	RETURN
#4	LOW	CW	3	22	5	-5	-. 23	RETURN
#3	LOW	CW	6	156	5	-5	- 03	VSWR
#1	HIGH	PULSED	1	158	100	+6, +8	+. 04, +. 05	MONITOR
#1	HIGH	PULSED	1	132, 122	100	-26, -18	-. 20, -. 15	RETURN
#3	LOW	CW	13	98	5	-7. 0	-. 07	RETURN
#4	LOW	CW	3	40	5	-4. 5	-. 11	RETURN
L ADAPTER #1 (POLYETHYLENE BEA	HIGH	PULSED	1	100, 95	100	+5, +5	+. 05, +. 05	RETURN
#3	LOW	CW	13	142	5	-10. 5	-. 07	RETURN
#4	LOW	CW	3	19	5	-5	-. 26	RETURN
#3	LOW	CW	6	198	5	-4. 5	-. 02	VSWR
#1	HIGH	PULSED	1	114, 86	100	--	--	RETURN
#3	LOW	CW	13	96	5	-10	-. 10	RETURN
#4	LOW	CW	3	20	5	-5. 5	-. 28	RETURN
#3	LOW	CW	6	162	5	-4. 5	-. 03	VSWR

1229B / 603P

PONDS TO THE HIGH POWER PULSE (P1
E SECOND VALUE CORRESPONDS TO

INT OF MEASUREMENT.

L.
E.
OM THE DEVICE.

PONENT UNDER TEST.
ENT UNDER TEST.

TABLE II. RESULTS OF RADIATION ENVIRONMENT T
WAVEGUIDE, COAXIAL ISOLATOR, COAXIAL CIRCULAT
UNDER 5.6 Gc R-F HIGH AND LOW POW

1	2	3	4	5	6		
IDENTIFICATION NO.	BURST NO.	BURST SIZE (°C)	INPUT NO.	COMPONENT UNDER TEST	DRIVING SIGNAL[4]		CI DE
1	9	93.5	8	ALUM. W/G (AIR FILLED)	LOW	CW	
2	10	111.5	8	ALUM. W/G (AIR FILLED)	LOW	CW	
3	17	104.0	8	ALUM. W/G (HI DENSITY POLY)	LOW	CW	
4	18	94.5	8	ALUM. W/G (HI DENSITY POLY)	LOW	CW	
5	14	84.0	2	ALUM. W/G (SOLID POLYETHYLENE)	LOW	CW	
6	15	90.5	2	ALUM. W/G (SOLID POLYETHYLENE)	LOW	CW	
7	16	94.0	2	ALUM. W/G (SOLID POLYETHYLENE)	LOW	CW	
8	5	109.0	8	COAXIAL ISOLATOR	LOW	CW	
9	6	102.8	8	COAXIAL ISOLATOR	LOW	CW	
10	15	90.5	6	COAXIAL CIRCULATOR	LOW	CW	
11	18	94.5	1	COAXIAL CIRCULATOR	HIGH	PULSE	
12	18	94.5	2	COAXIAL CIRCULATOR	HIGH	PULSE	
13	12	98.0	11	COAXIAL LIMITER	LOW	CW	
14	18	94.5	4	COAXIAL LIMITER	LOW	CW	
15	15	90.5	1	COAXIAL LIMITER	HIGH	PULSED	

NOTES:
1. WHERE THERE ARE TWO VALUES GIVEN, THE FIRST CORRESPONDS TO THE HIGH POWER PULSE (PI) DELAYED ~ 200 μ SECONDS AFTER THE SPR TRIGGER; AND THE SECOND VALUE CORRESPONDS TO THE PULSE (P2) ~ 350 μ SECONDS AFTER THE SPR TRIGGER.
2. POSITIVE SIGNS INDICATED AN INCREASE IN POWER AT THE POINT OF MEASUREMENT.
3. MONITOR: DETECTOR MONITORING THE INPUT SIGNAL LEVEL.
   VSWR: DETECTOR MONITORING THE VSWR OF THE DEVICE.
   RETURN: DETECTOR MONITORING THE RETURN SIGNAL FROM THE DEVICE.
4. LOW CW, APPROXIMATELY 100 MILLIWATTS CW AT THE COMPONENT UNDER TEST. HIGH PULSED, APPROXIMATELY 5 KW AT THE COMPONENT UNDER TEST.

* SAME MAGNITUDE OBSERVED DURING BURST 13.

1

TABLE II. RESULTS OF RADIATION ENVIRONMENT TESTING OF ALUMINUM WAVEGUIDE, COAXIAL ISOLATOR, COAXIAL CIRCULATOR, AND COAXIAL LIMITER UNDER 5.6 Gc R-F HIGH AND LOW POWER CONDITIONS

5	6	7	8	9	10	11	12
COMPONENT UNDER TEST	[illegible] SIGNAL[4]	CRYSTAL DETECTOR NO.	CRYSTAL SENSITIVITY (MV/DB)	VERTICAL GAIN (MV/CM)	MAGNITUDE OF EFFECT (MV)[1,2]	MAGNITUDE OF EFFECT (DB)[1,2]	SIGNAL[3]
ALUM. W/G (AIR FILLED)	CW	3	28	5	-10.2	-.36	RETURN
ALUM. W/G (AIR FILLED)	CW	3	160	5	-20.3	-.13	RETURN
ALUM. W/G (HI DENSITY POLY)	CW	3	66	5	-13.5	-.21	RETURN
ALUM. W/G (HI DENSITY POLY)	CW	3	60	5	-12.2	-.20	RETURN
ALUM. W/G (SOLID POLYETHYLENE)	CW	3	75	5	-3	-.04	RETURN
ALUM. W/G (SOLID POLYETHYLENE)	CW	3	80	5	-3	-.04	RETURN
ALUM. W/G (SOLID POLYETHYLENE)	CW	3	100	5	-4	-.04	RETURN
COAXIAL ISOLATOR	CW	3	42	5	-4.5	-.11	RETURN
COAXIAL ISOLATOR	CW	3	86	5	-7.2	-.08	RETURN
COAXIAL CIRCULATOR	CW	12	100	5	2	0.02	ANTENNA RETURN
COAXIAL CIRCULATOR	PULSE	14	144, 101	100	+20, +20	+.14, +.20	MONITOR
COAXIAL CIRCULATOR	PULSE	1	8, 6	5	0.5, 0.5	+0.06, +0.1	ANTENNA RETURN
COAXIAL LIMITER	CW	6	364	20	-6.0	-.02*	RETURN
COAXIAL LIMITER	CW	13	62	5	-5.5	-.09	RETURN
COAXIAL LIMITER	PULSED	1	240	2000	+2600	+10	RETURN

S GIVEN, THE FIRST CORRESPONDS TO T
D 200 SECONDS AFTER THE SPR TR
SPONDS TO THE PULSE (P2) - 350 μ SEC-

NCREASE IN POWER AT THE POINT OF

RING THE INPUT SIGNAL LEVEL.
RING THE VSWR OF THE DEVICE.
RING THE RETURN SIGNAL FROM THE DE

MILLIWATTS CW AT THE COMPONENT U
MATELY 5 KW AT THE COMPONENT UND

RING BURST IS

2

TABLE III. RESULTS OF RADIATION ENVIRONMENT TESTING OF OPERATING AT 5.6 GC AT HIGH AND LOW R-F POWER

1 IDENTIFICATION NO.	2 BURST NO.	3 BURST SIZE (C)	4 INPUT NO.	5 COMPONENT UNDER TEST	6 DRIVING SIGNAL[4]		7 CRYSTAL DETECTOR NO
1	5	109.0	6	COAXIAL DUPLEXER	LOW	CW	12
2	6	102.8	6		LOW	CW	12
3	6	102.8	10		LOW	CW	11
4	7	97.5	6		LOW	CW	12
5	8	100.5	6		LOW	CW	12
6	8	100.5	10		LOW	CW	11
7	9	93.5	1		HIGH	PULSE	14
8	9	93.5	2		HIGH	PULSE	1
9	10	111.5	1		HIGH	PULSE	14
10	10	111.5	2	COAXIAL DUPLEXER	HIGH	PULSE	1

NOTES:

1. WHERE THERE ARE TWO VALUES GIVEN, THE FIRST CORRESPONDS TO THE HIGH POWER PULSE (P1) DELAYED ~ 200 μ SECONDS AFTER THE SPR TRIGGER; AND THE SECOND VALUE CORRESPONDS TO THE PULSE (P2) ~ 350 μ SECONDS AFTER THE SPR TRIGGER.
2. POSITIVE SIGNS INDICATE AN INCREASE IN POWER AT THE POINT OF MEASUREMENT.
3. MONITOR: DETECTOR MONITORING THE INPUT SIGNAL LEVEL.
   VSWR: DETECTOR MONITORING VSWR OF THE DEVICE.
   RETURN: DETECTOR MONITORING THE RETURN SIGNAL FROM THE DEVICE.
4. LOW CW, APPROXIMATELY 100 MILLIWATTS CW
   HIGH PULSED, APPROXIMATELY 5 KW PEAK.

TABLE III. RESULTS OF RADIATION ENVIRONMENT TESTING OF THE COAXIAL DUPLEXER OPERATING AT 5.6 GC AT HIGH AND LOW R-F POWER CONDITIONS

3 T	4 BURST SUP	5 INPUT NO.	COMPONENT	UNIT	6 DRIVING SIGNAL[4]		7 CRYSTAL DETECTOR NO.	8 CRYSTAL SENSITIVITY (MV DB)	9 VERTICAL GAIN (MV CM)	10 MAGNITUDE OF EFFECT (MV)[1, 2]	11 MAGNITUDE OF EFFECT (DB)[1, 2]	12 SIGNAL[3]
	[illegible]	3	COAXIAL	[illegible]	LOW	CW	12	78	5	-5.5	-.07	ANTENNA RETURN
	[illegible]	4			LOW	CW	12	78	5	-5.0	- 06	ANTENNA RETURN
	[illegible]	10			LOW	CW	11	12	5	-2.8	-.23	RECEIVER RETURN
	[illegible]	9			LOW	CW	12	68	5	-5.0	-.07	ANTENNA RETURN
	[illegible]	6			LOW	CW	12	73	5	-5.1	-.07	ANTENNA RETURN
	[illegible]	10			LOW	CW	11	15	50	-3.0	-0.2	RECEIVER RETURN
	[illegible]	3			HIGH	PULSE	14	160, 180	100	-24, -26	- 15, -.14	MONITOR
	[illegible]	9			HIGH	PULSE	1	96, 107	100	-6	+.06	ANTENNA RETURN
	[illegible]	9			HIGH	PULSE	14	178, 194	100	-28, -34	-.16, -.18	MONITOR
	[illegible]	3	COAXIAL	[illegible]	HIGH	PULSE	1	142, 148	100	-16, -16	-.11, - 11	ANTENNA RETURN

[illegible]/[illegible]

[illegible] HERE ARE TWO VALUES GIVEN, THE F[illegible] ORRESPONDS TO
[illegible] POWER PULSE (PD) DELAYED 200 [illegible] ONDS AFTER THE
[illegible] GER AND THE SECOND VALUE CORRE[illegible] TO THE PULSE
SECONDS AFTER THE SPR TRIGGER.

[illegible] SIGNS INDICATE AN INCREASE IN POW[illegible] THE POINT OF
[illegible] MENT

[illegible] DETECTOR MONITORING THE INPUT[illegible] LEVEL.
[illegible] DETECTOR MONITORING VSWR OF T[illegible] AGE
[illegible] DETECTOR MONITORING THE REFLE[illegible] ED FROM THE
[illegible] DEVICE

[illegible] APPROXIMATELY [illegible] MILLIWATTS[illegible]
[illegible] APPROXIMATELY [illegible] KW PEAK.

4-15/16

2

TABLE IV. RESULTS OF RADIATION ENVIRONMENT TES
CIRCULATOR AND A WAVEGUIDE PHASE-SHIFT TYPE
5.6 Gc R-F HIGH AND LOW POWER CONDITI

1	2	3	4	5	6		7
IDENTIFICATION NO.	BURST NO.	BURST SIZE (°C)	INPUT NO.	COMPONENT UNDER TEST	DRIVING SIGNAL[4]		CRYSTAL DETECTOR NO.
1	5	109.0	4	W G CIRCULATOR	LOW	CW	13
2	6	102.8	4		LOW	CW	13
3	9	93.5	4		LOW	CW	13
4	9	93.5	11		LOW	CW	6
5	10	111.5	4		LOW	CW	13
6	11	95.0	1		HIGH	PULSE	14
7	11	95.0	2		HIGH	PULSE	1
8	12	98.0	1		HIGH	PULSE	14
9	12	98.0	2		HIGH	PULSE	1
10	13	96.5	1		HIGH	PULSE	14
11	13	96.5	2		HIGH	PULSE	1
12	14	84.0	4		LOW	CW	2
13	15	90.5	4		LOW	CW	2
14	16	94 0	4		LOW	CW	2
15	17	104.0	3		LOW	CW	7
16	17	104.0	4		LOW	CW	2
17	17	104.0	11	W G CIRCULATOR	LOW	CW	6

NOTE: 1 WHERE TWO VALUES ARE GIVEN, THE FIRST CORRESPONDS TO THE HIGH POWER PULSE (P1) DELAYED ~200 μ SECONDS AFTER THE SPR TRIGGER; AND THE SECOND VALUE CORRESPONDS TO THE PULSE (P2) ~350 μ SECONDS AFTER THE SPR TRIGGER.

2 POSITIVE SIGNS INDICATE AN INCREASE IN POWER AT THE POINT OF MEASUREMENT

3 MONITOR: DETECTOR MONITORING THE INPUT SIGNAL
VSWR: DETECTOR MONITORING THE VSWR OF THE DEVICE
RETURN: DETECTOR MONITORING THE RETURN SIGNAL FROM THE DEVICE

4 LOW CW, APPROXIMATELY 100 MILLIWATTS CW. HIGH PULSED, APPROXIMATELY 5KW PEAK

TABLE IV. RESULTS OF RA[illegible]ION ENVIRONMENT TESTING OF A WAVEGUIDE CIRCULATOR AND A W[illegible]VEGUIDE PHASE-SHIFT TYPE DUPLEXER UNDER 5.6 Gc R-F HIGH [illegible]ND LOW POWER CONDITIONS (SHEET 1)

4 INPUT NO.	5 COMPONENT UNDER TEST	6 [illegible]G SIGNAL[4]	7 CRYSTAL DETECTOR NO.	8 CRYSTAL SENSITIVITY (MV DB)	9 VERTICAL GAIN (MV CM)	10 MAGNITUDE OF EFFECT (MV)[1, 2]	11 MAGNITUDE OF EFFECT (DB)[1, 2]	12 SIGNAL[3]
4	W G CIRCULATOR	CW	13	90	5	-14.5	-.16	ANTENNA RETURN
4		CW	13	96	10	-14.6	-.15	ANTENNA RETURN
4		CW	13	98	5	-11.9	-.12	ANTENNA RETURN
11		CW	6	--	10	-3.4	--	VSWR
4		CW	13	111	5	-16.9	-.15	ANTENNA RETURN
1		PULSE	14	157, 174	100	-6, -6	-.04, -.03	MONITOR
2		PULSE	1	50, 218	20	+5.2, +5.2	+.10, +.02	ANTENNA RETURN
1		PULSE	14	156, 160	100	-4, -4	-.03, -.03	MONITOR
		PULSE	1	56, 46	50	-6, -5	-.11, -.11	ANTENNA RETURN
1		PULSE	14	196, 193	100	-4, +4	-.02, +.02	MONITOR
2		PULSE	1	54, 59	50	-4,	-.07,	ANTENNA RETURN
4		CW	2	78	5	-7	-.09	ANTENNA RETURN
4		CW	2	86	5	-8.5	-.10	ANTENNA RETURN
3		CW	2	95	5	-10.6	-.11	ANTENNA RETURN
		CW	7	78	5	-5.0	-.06	MONITOR
3		CW	2	92	5	-14.0	-.15	ANTENNA RETURN
11	W G CIRCULATOR	CW	6	--	10	-4.0	--	VSWR

EN, THE FIRST CORRESPONDS TO THE HI[illegible]OWER
ECONDS AFTER THE SPR TRIGGER; AND [illegible] SECOND
PULSE (T2 = 350 μ SECONDS AFTER THE [illegible] TRIGGER.

NCREASE IN POWER AT THE POINT OF M[illegible]EMENT

RING THE INPUT SIGNAL
G THE VSWR OF THE DEVICE
RING THE RETURN SIGNAL FROM THE DE

0 MILLIWATTS CW HIGH PULSED, APPR[illegible]MATELY

**TABLE IV. RESULTS OF RADIATION ENVIRONMENT TESTI
CIRCULATOR AND A WAVEGUIDE PHASE-SHIFT TYPE
5.6 Gc R-F HIGH AND LOW POWER CONDITIO**

1	2	3	4	5	6		7
IDENTIFICATION NO.	BURST NO.	BURST SIZE (°C)	INPUT NO.	COMPONENT UNDER TEST	[illegible] SIGNAL[4]		CRYSTAL DETECTOR NO.
18	1	96.5	10	W G DUPLEXER	[illegible]	CW	15
19	2	96.0	6		[illegible]	CW	12
20	2	96.0	10		[illegible]	CW	15
21	3	105.5	6		[illegible]	CW	12
22	3	105.5	10		[illegible]	CW	15
23	4	106.2	6		[illegible]	CW	12
24	4	106.2	10		[illegible]	CW	15
25	5	109.0	1		[illegible]	PULSE	8
26	5	109.0	2		[illegible]	PULSE	1
27	6	102.8	1		[illegible]	PULSE	8
28	6	102.8	2		[illegible]	PULSE	1
29	7	97.5	1		[illegible]	PULSE	8
30	7	97.5	2		[illegible]	PULSE	1
31	8	100.5	1		[illegible]	PULSE	8
32	8	100.5	2		[illegible]	PULSE	1
33	9	93.5	6		[illegible]	CW	12
34	10	111.5	6		[illegible]	CW	12
35	11	95.0	8		[illegible]	CW	3
36	12	98.0	8	W G DUPLEXER	[illegible]	CW	3

NOTE 1 WHERE TWO VALUES ARE GIVEN, THE FIRST CORRESPONDS TO THE HIGH POWER PULSE (P1) DELAYED ~ 200 μ SECONDS AFTER THE SPR TRIGGER; AND THE SECOND VALUE CORRESPONDS TO THE PULSE (P2) ~ 350 μ SECONDS AFTER THE SPR TRIGGER.

2 POSITIVE SIGNS INDICATE AN INCREASE IN POWER AT THE POINT OF MEASUREMENT.

3. MONITOR: DETECTOR MONITORING THE INPUT SIGNAL
VSWR: DETECTOR MONITORING THE VSWR OF THE DEVICE
RETURN: DETECTOR MONITORING THE RETURN SIGNAL FROM THE DEVICE

4 LOW CW, APPROXIMATELY 100 MILLIWATTS CW, HIGH PULSED, APPROXIMATELY 5KW PEAK

TABLE IV. RESULTS OF RAD[illegible] ENVIRONMENT TESTING OF A WAVEGUIDE CIRCULATOR AND A WA[illegible] OF PHASE-SHIFT TYPE DUPLEXER UNDER 5.6 GC R-. HIGH A[illegible] W POWER CONDITIONS (SHEET 2)

	COMPONENT UNDER TEST		[illegible]AL[4]	7 CRYSTAL DETECTOR NO.	8 CRYSTAL SENSITIVITY (MV/DB)	9 VERTICAL GAIN (MV/CM)	10 MAGNITUDE OF EFFECT (MV)[1,2]	11 MAGNITUDE OF EFFECT (DB)[1,2]	12 SIGNAL[3]
	[illegible] DUPLEXER		[illegible]	15	30	5	-19.8	- 66	RECEIVER RETURN
			[illegible]	12	108	5	-15.1	- 14	ANTENNA RETURN
			[illegible]W	15	73	10	-38.0	- 52	RECEIVER RETURN
			[illegible]W	12	107	10	-22.0	- 21	ANTENNA RETURN
			[illegible]W	15	60	10	-30.0	-.50	RECEIVER RETURN
			[illegible]W	12	100	10	-22.0	- 22	ANTENNA RETURN
			[illegible]W	15	66	10	-34.0	- 52	RECEIVER RETURN
		H[illegible]	PULSE	8	220, 226	100	+20, +20	+0.1, +0.1	MONITOR
		H	PULSE	1	180, 170	100	-18, -10	-.09, -.09	ANTENNA RETURN
		H	PULSE	8	200, 212	100	+20, +22	+.10, +.10	MONITOR
		H	PULSE	1	156, 148	100	-22, -22	- 14, - 15	ANTENNA RETURN
		H	PULSE	8	182, 206	100	+18, +20	+ 10, +.10	MONITOR
		H	PULSE	1	145, 137	100	-16, -10	-.11, -.07	ANTENNA RETURN
		H	PULSE	8	186, 190	100	+30, +38	+.16, +.20	MONITOR
		H	PULSE	1	96, 104	100	15, -16	- 15, - 15	ANTENNA RETURN
			[illegible]	12	73	5	-11 7	16	ANTENNA RETURN
			[illegible]W	12	83	5	-15.9	- 19	ANTENNA RETURN
			[illegible]	3	76	5	-12 0	- 15	ANTENNA RETURN
	[illegible] DUPLEXER		[illegible]	3	52	5	-12 [illegible]	- 24	ANTENNA RETURN

THE FIRST CORRESPONDS TO THE HIGH [illegible]
[illegible]ONDS AFTER THE SPR TRIGGER; AND TH[illegible]
[illegible] SECONDS AFTER THE S[illegible]

[illegible] POWER AT THE POINT OF MEA[illegible]

[illegible] THE INPUT SIGNAL
[illegible] OF THE DEVICE
[illegible] RETURN SIGNAL FROM THE DEV[illegible]

[illegible] PULSED APPROX[illegible]

2

TABLE V. SPRF BURST DATA FOR THE FIF[illegible] SPERRY MICROWAVE ELECTRONICS COMPANY EXPERIM[illegible]NTAL TESTS

S.P.R.F. BURST NO.	S.M.E.C BURST NO.	DATE	TIME	[illegible]	TOTAL NO. FISSIONS
12-1	1	12-2-63	[illegible]	[illegible]	1.76×10^{16}
12-2	[illegible]	[illegible]	[illegible]	[illegible]	[illegible]
[illegible]	[illegible]	[illegible]	[illegible]	[illegible]	1.92×10^{16}
12-4	[illegible]	[illegible]	[illegible]	[illegible]	1.93×10^{16}
12-5	5	[illegible]	[illegible]	[illegible]	1.98×10^{16}
12-6	6	[illegible]	[illegible]	102.8	1.87×10^{16}
12-7	7	[illegible]	[illegible]	[illegible]	[illegible]
12-8	[illegible]	[illegible]	[illegible]	[illegible]	1.83×10^{16}
12-9	9	12-3-63	[illegible]	[illegible]	1.70×10^{16}
12-10	10	[illegible]	[illegible]	[illegible]	2.05×10^{16}
[illegible]	[illegible]	[illegible]	[illegible]	[illegible]	1.73×10^{16}
12-12	[illegible]	[illegible]	[illegible]	[illegible]	[illegible]
[illegible]	[illegible]	[illegible]	[illegible]	[illegible]	1.76×10^{16}
[illegible]	[illegible]	[illegible]	1600	[illegible]	[illegible]
[illegible]	[illegible]	[illegible]	[illegible]	[illegible]	1.66×10^{16}
[illegible]	[illegible]	[illegible]	[illegible]	[illegible]	1.71×10^{16}
[illegible]	[illegible]	[illegible]	[illegible]	[illegible]	1.89×10^{16}
[illegible]	[illegible]	[illegible]	15	[illegible]	[illegible]
[illegible]	[illegible]	[illegible]	[illegible]	[illegible]	1.80×10^{16}
[illegible]	[illegible]	[illegible]	[illegible]	[illegible]	1.69×10^{16}

- Under the same conditions, the average transient decrease in signal level passing through the adapters using polyethylene beads was less than 0.2 db or approximately twice that of the Rexolite beads.

- No significantly different results were observed when operating under high pulsed r-f power conditions.

Aluminum Waveguide Sections. A one-foot aluminum waveguide section (using waveguide-to-coaxial adapters, Rexolite beads), air filled, solid polyethylene filled, and high density polyfoam filled, was evaluated at low power. Using the same adapters, the average transient decrease in signal level through the air filled and high density polyfoam filled waveguide was approximately the same at 0.2 db. The solid dielectric polyethylene reduced the observed effects to 0.04 db. The data are tabulated in Table II.

Coaxial Isolator. The data in Table II conclude that the average transient increase in insertion loss of the coaxial isolators tested is 0.1 db at low power and 5.6 Gc. This is a value somewhat higher than the 0.02 db reported in the Sixth Quarterly Report.[6]

Coaxial Circulator. The coaxial circulator, according to Table II, exhibited an average transient increase in insertion loss of 0.02 db. This is in good agreement with data previously taken on this component. The tests were performed at approximately 100 milliwatts at 5.6 Gc. No significant transient effects were observed while the component was operating under high power.

Coaxial Limiter. The following conclusions were reached from Table II regarding the coaxial limiter tests:

- The average transient increase in the insertion loss of the coaxial limiter operating at approximately 100 milliwatts was 0.02 db. (This is in good agreement with previous data.)[6]
- The average transient decrease in the insertion loss, i.e., increase in the signal from the coaxial limiter operating at approximately 5 Kw, was greater than 10 db.

When operating at low power, the coaxial limiter is operating below the threshold limiting level; therefore, at this power level, it may be expected to show an increase in insertion loss due to ionization which the tests substantiated. When the limiter was operated at 5 Kw, however, the limiter is operating above the limiting threshold. It is reasonable to assume that the pulsed radiation on the component may deteriorate the limiting action. The tests indicated that the limiting action of the device was

temporarily deteriorated to a great extent upon exposure to radiation while operating at high power levels.

A full explanation of cause of the large transient effects observed in the limiter are not presently formulated. As mentioned previously in Section 4.1.6, both limiters tested at the SPRF apparently were in a non-operating condition even at low power just after the high power r-f tests in the pulsed radiation environment.

These limiters were rechecked at low and high r-f power (no radiation environment) approximately two months later and seem to be in normal operating conditions. The typical measured operating characteristics at low power are shown in Figure 19.

The limiter exhibited apparent normal operating characteristics at high power in these tests two months after evaluation in the radiation environment. The limiting characteristics are depicted in Figure 20. Examination of the structure revealed no evidence of r-f arcing.

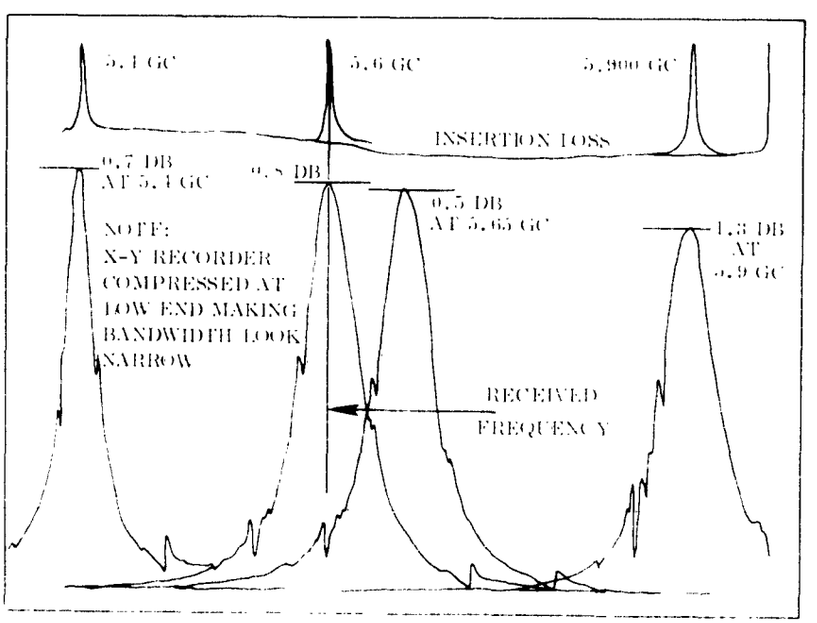

Figure 19. Low power characteristics of gyromagnetic coupling limiter, Serial No. 1, approximately two months after pulsed radiation tests.

Since radiation damage thresholds in ferrimagnetic ceramic materials have been measured to be quite high (approximately 10^{20} neutrons cm^2), the observed effects are not attributed to changes in the characteristics of the single crystal yttrium iron garnet material used in the limiter.

The limiter is a fine tuned device as shown in Figure 19. Any changes in the magnetic biasing field strongly affects the r-f signal coupled through the limiter. It is expected though that any changes of this type (similar effects would be noted as a function of temperature) would reduce the output signal of the limiter. However, any signal changes due to alterations in the magnetic biasing field should occur at both high and low power.

The limiter is composed of two crossed, very narrow strips between which the r-f energy is coupled by a small (0.023" diameter O. D.) single crystal sphere of yttrium iron garnet magnetically biased to ferrimagnetic resonance at the operating frequency. Normally, all of the r-f energy passing from the input strip to the output strip must be coupled through the sphere. The sphere is encapsulated in a teflon holder which also spaces the strips approximately 0.030" apart. The radiation test data indicate that during the nuclear burst, energy is coupled directly from strip to strip, bypassing the yttrium iron garnet coupling sphere. In other terms, the dynamic range (limiting range) of the limiter seems to decrease. However, no pulse radiation data have been collected between the 100 milliwatt r-f power level and the 5 Kw level to verify this.

The apparent permanent damage and then recovery is somewhat puzzling unless the characteristics of the teflon sphere holder and spacer are temporarily altered

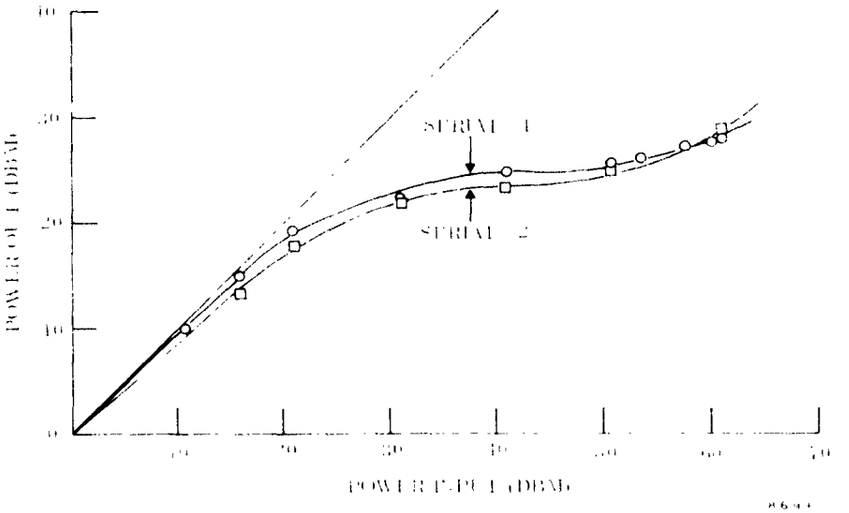

Figure 20. Limiting characteristics of coaxial limiters taken approximately two months after pulsed radiation tests.

due to the radiation. However, evidence of any effects such as this should also have been observed in low r-f power experiments. Low power tests have always indicated very small transient effects. The coincidence of the high r-f peak power and the pulsed nuclear radiation seems necessary to produce the undesirable operating characteristics.

Redesign of the limiter structure itself may be required to eliminate the observed transient effects at high r-f power.

Coaxial Duplexer-Limiter. The following conclusions are offered from the data of Table III concerning the coaxial duplexer tested:

- The average transient increase in insertion loss of the coaxial duplexer operating at approximately 100 milliwatts was 0.07 db (in agreement with previous results).
- The average transient decrease in the signal level from the receiver port of the coaxial duplexer operating at approximately 100 milliwatts was 0.2 db.
- The average transient decrease in insertion loss of the coaxial duplexer operating at approximately 5 Kw was less than 0.2 db for P1 or P2.

The level of the signal from the receiver port (through gyromagnetic coupling limiter) did not increase as noted for the individual tests on the limiter because of the low level of the r-f signal incident at the limiter. This port is isolated by approximately 30 db from the input signal.

Waveguide Junction Circulator. The data in Table IV regarding the waveguide circulator indicate the following conclusions:

- The average transient increase in the insertion loss of the waveguide circulator operating approximately 100 milliwatts at 5.6 Gc was 0.13 db (approximately twice that reported in the Sixth Quarterly Report).
- The average transient increase in the insertion loss of the waveguide circulator operating at approximately 5 Kw at 5.6 Gc was less than 0.1 db (approximately the same as at low power).
- No significant changes were observed in the signal level from the receiver port. (See Figure 9.)

Waveguide Differential Phase Shift Duplexer. Following are the conclusions reached from the data of Table IV on the waveguide duplexer:

- The average transient increase in insertion loss (antenna return) of the waveguide duplexer operating at low power (approximately 100 milliwatts) at 5.6 Gc was less than 0.2 db.

- The average transient decrease in isolation (receiver return) of the waveguide duplexer operating at low power (approximately 100 milliwatts cw) at 5.6 Gc was 0.5 db.

- The average transient increase in the insertion loss (antenna return) of the waveguide duplexer operating at approximately 5 Kw peak at 5.6 Gc was less than 0.25 db (essentially the same as observed at low power).

The transient effects observed for both the waveguide circulator and waveguide duplexer are near the magnitude observed for the adapters as reported previously. A waveguide-to-coaxial adapter is required on each port of these components when performing tests at the SPRF.

4.3 DOSIMETRY

The burst magnitude data provided by the SPRF personnel at the time of the experiments are summarized in Table V. The change in bulk reactor temperature during the burst is given with the total number of fissions which occurred during the burst. The latter parameter is calculated by means of the following relation:[7]

$$\text{Total number of fissions} = \frac{\Delta T\ (^{\circ}C)}{55} \times 10^{16}.$$

The dosimetry support given by the Sandia Corporation Nuclear Measurements and Dosimetry Section consisted of the following:

(a) Four sulfur pellets per burst to measure the integrated neutron ($E_n > 3.00$ Mev) flux at each component.

(b) One or two each per day of pultonium, neptunium, and uranium fission foils enclosed in a boron ball to measure the integral neutron fluxes where

$E_n > 0.01$ Mev for Pu threshold

$E_n > 0.7$ Mev for Np threshold

$E_n > 1.5$ Mev for U threshold

(c) Two gold foils for each burst, one of which was cadmium covered, to measure the integrated neutron ($E_n > 0.4$ ev) flux.

(d) One glass rod (in lithium cylinders) per burst to measure the integrated γ-ray dose in rads H_2O. (In this definition 1 rad is the amount of γ radiation necessary to produce a 100 erg/gram energy absorption rate in water.)

One to two sets of fission foils (item b) were used per day of testing. The $E_n > 0.01$ Mev, $E_n > 0.7$ Mev and $E_n > 1.5$ Mev integral fluxes for the other bursts obtained that day may be determined from the values measured during the burst in which the foils were present by interpolation provided the total mass surrounding the reactor is not changed appreciably. A ratio of burst to burst integral fluxes ($E_n > 3.0$ Mev), as measured by the sulfur pellets, may be used to calculate the equivalent fission foil fluxes for the other bursts obtained during the day. This procedure was suggested by SPRF personnel.[8]

To obtain the maximum dose rates from the integral quantities reported by the Nuclear Measurements and Dosimetry Section, the following procedure[9] was followed. The reactor period associated with the burst is denoted by T. The width of the neutron pulse at one-half maximum, Tw, is given by Tw = 2.86T. For a 50-microsecond wide pulse, the period is 1.75×10^{-5} seconds or 17.5 microseconds. The reciprocal reactor period $\alpha = 1/T$ is 5.72×10^{4} sec^{-1}. The ratio of peak fission rate to total fissions is

$$\frac{F_{max}}{F_{total}} = \frac{\alpha}{4} = 1.43 \times 10^{4}/\text{second for a 50 } \mu\text{sec pulse.}$$

The neutron flux above 3.0 Mev is measured by sulfur pellets, which is about 14.5 percent of the total flux above 10 Kev. The first collision tissue dose is related to the sulfur flux by $D_n = 1.66 \times 10^{-8} \phi_s$. About 80 percent of the total neutron dose is delivered during the prompt critical burst and the remaining 20 percent during the delayed critical portion of the burst.

Approximately 75 percent of the total gamma dose is delivered during the prompt critical burst, and the total gamma dose is approximately 10 percent of the total neutron dose. The peak gamma dose rate then becomes $1.9 \times 10^{-2} D_n/T$, where D_n is the total neutron dose delivered during the burst and T is the reactor period. The results of these type calculations giving dose rates along with the integral doses, where available, are given in Table VI (which appears at the end of this section).

4.4 SUMMARY OF RESULTS

Table VI presents a summary of all the radiation transient effects observed together with the dosimetry report (magnitude of radiation burst) for each component tested.

SYMBOL DEFINITIONS FOR TABLE VI

S = DIFFERENCE BETWEEN CENTER OF RADIATION BURST AND CENTER OF P1 (MICROSECONDS)

E_{ns} = INTEGRATED NEUTRON FLUX 3.0 Mev (NEUTRONS/cm^2)

$E_n 1.5$ = INTEGRAL NEUTRON FLUX 1.5 Mev (NEUTRONS/cm^2)

$= \frac{E_{ns}}{.145}$

$E_n 0.6$ = INTEGRAL NEUTRON FLUX 0.7 Mev (NEUTRONS/cm^2)

$E_n 0.01$ = INTEGRAL NEUTRON FLUX 0.01 Mev (NEUTRONS/cm^2)

D_n = FIRST COLLISION TISSUE DOSE OF NEUTRONS (RADS)

$= 1.66 \times 10^{-8} E_{ns}$ WHERE 1.66×10^{-8} IS AN EMPIRICAL NUMBER

T_w = RADIATION PULSE WIDTH AT ONE-HALF MAXIMUM OBTAINED FROM SPRF PHOTOGRAPH (SECONDS)

T = REACTOR PERIOD = $\frac{1}{2.86} T_w$ WHERE $\frac{1}{2.86}$ IS AN EMPIRICAL NUMBER (SEC.)

R = RATIO OF PEAK NEUTRON FISSION RATE TO THE TOTAL NEUTRON FISSIONS = $\frac{1}{4T}$

D_g = INTEGRATED GAMMA DOSE (RADS)

D_{gr} = PEAK GAMMA DOSE RATE (RADS/SEC.)

NOTES:

* Power level delivered to the component under test { Hi pulsed ~ 5 kw / Low cw ~ 100 milliwatts

** Positive sign indicates the center of the radiation burst was ahead of the center of P1.

*** $E_n 0.01$ was calculated assuming $E_{ns} = 0.145 E_n 0.01$.

TABLE VI

RADIATION BURST AND

ev (NEUTRONS cm^2)

(NEUTRONS cm^2)

(NEUTRONS cm^2)

(NEUTRONS cm^2)

EUTRONS (RADS)

AN EMPIRICAL NUMBER

ALF MAXIMUM OBTAINED

RE $\frac{1}{2.86}$ IS AN EMPIRICAL

ATE TO THE TOTAL NEUTRON

C.)

onent under test $\begin{cases} \text{Hi pulsed} \sim 5\,\text{kw} \\ \text{Low cw} \sim 100\ \text{milliwatts} \end{cases}$

of the radiation burst was ahead

$E_{ns} = 0.145\ E_n\ 0.01.$

1 BURST NUMBER	2 COMPONENT EXPOSED	3 POWER LEVEL *	4 S ** (MICROSECONDS)	5 INTEGRATED NEUTRON FLUX E_{ns} (NEUTRONS, cm^2)
1	W/G TO COAXIAL ADAPTER #1 (REXOLITE BEAD)	HI PULSED	0	1.05×10^{12}
	W/G TO COAXIAL ADAPTER #3 (REXOLITE BEAD)	LOW CW		1.36×10^{12}
	W/G TO COAXIAL ADAPTER #4 (REXOLITE BEAD)	LOW CW		1.35×10^{12}
	W/G DUPLEXER	LOW CW		1.65×10^{12}
2	W/G TO COAXIAL ADAPTER #1 (REXOLITE BEAD)	HI PULSED	0	5.59×10^{11}
	W/G TO COAXIAL ADAPTER #3 (REXOLITE BEAD)	LOW CW		1.28×10^{12}
	W/G TO COAXIAL ADAPTER #4 (REXOLITE BEAD)	LOW CW		1.67×10^{12}
	W/G DUPLEXER	LOW CW		1.60×10^{12}
3	W/G TO COAXIAL ADAPTER #1 (POLYETHYLENE BEAD)	HI PULSED	+15	6.17×10^{11}
	W/G TO COAXIAL ADAPTER #3 (POLYETHYLENE BEAD)	LOW CW		1.11×10^{12}
	W/G TO COAXIAL ADAPTER #4 (POLYETHYLENE BEAD)	LOW CW		1.10×10^{12}
	W/G DUPLEXER	LOW CW		1.91×10^{12}
4	W/G TO COAXIAL ADAPTER #1 (POLYETHYLENE BEAD)	HI PULSED	+20	5.55×10^{11}
	W/G TO COAXIAL ADAPTER #3 (POLYETHYLENE BEAD)	LOW CW		1.11×10^{12}
	W/G TO COAXIAL ADAPTER #4 (POLYETHYLENE BEAD)	LOW CW		1.21×10^{12}
	W/G DUPLEXER	LOW CW		1.64×10^{12}
5	W/G DUPLEXER	HI PULSED	+20	1.73×10^{12}
	W/G CIRCULATOR	LOW CW		2.05×10^{12}
	COAXIAL DUPLEXER	LOW CW		1.43×10^{12}
	COAXIAL ISOLATOR	LOW CW		1.43×10^{12}
6	W/G DUPLEXER	HI PULSED	0	1.52×10^{12}
	W/G CIRCULATOR	LOW CW		1.38×10^{12}
	COAXIAL DUPLEXER	LOW CW		2.14×10^{12}
	COAXIAL ISOLATOR	LOW CW		1.38×10^{12}
7	W/G DUPLEXER	HI PULSED	0	1.55×10^{12}
	COAXIAL DUPLEXER	LOW CW		2.12×10^{12}
8	W/G DUPLEXER	HI PULSED	0	1.67×10^{12}
	COAXIAL DUPLEXER	LOW CW		2.08×10^{12}

TABLE VI. NEUTRON AND γ-RAY DOSIMETRY PROVIDING INTEGRAL DOSE AND DOSE RA
TO THE MICROWAVE COMPONENTS AND THE OBSERVED EFFECTS (SHEET 1)

3	4	5	6	7	8	9	10	11	12
POWER LEVEL *	** MICROSECONDS	INTEGRATED NEUTRON FLUX E_{ns} (NEUTRONS/cm^2)	INTEGRATED NEUTRON FLUX (BORON BALL) (NEUTRONS/cm^2)			INTEGRATED NEUTRON FLUX *** E_n 0.01 (CALCULA[illegible]) (NEUTRONS cm^{-2})	NEUTRON TISSUE DOSE D_n (RADS)	PULSE WIDTH T_w (SEC.)	REAC PERI T (SE
			E_n 1.5	E_n 0.6	E_n 0.01				
HI PULSED		1.05×10^{12}	2.25×10^{12}	4.44×10^{12}	6.32×10^{12}	7.24×10^{12}	1.74×10^{4}	41×10^{-6}	14.3 x
LOW CW		1.36×10^{12}				9.38×10^{12}	2.26×10^{4}	41×10^{-6}	14.3 x
LOW CW		1.35×10^{12}				9.31×10^{12}	2.24×10^{4}	41×10^{-6}	14.3 x
LOW CW		1.65×10^{12}				1.14×10^{13}	2.74×10^{4}	41×10^{-6}	14 .
HI PULSED		6.59×10^{11}				4.54×10^{12}	1.09×10^{4}	40×10^{-6}	14.0 x
LOW CW		1.28×10^{12}				8.83×10^{12}	2.12×10^{4}	40×10^{-6}	14.0 x
LOW CW		1.67×10^{12}				1.15×10^{13}	2.77×10^{4}	40×10^{-6}	14.0 x
LOW CW		1.60×10^{12}				1.10×10^{13}	2.66×10^{4}	40×10^{-6}	14.0 x
HI PULSED		6.17×10^{11}				4.26×10^{12}	1.02×10^{4}	40×10^{-6}	14.0 x
LOW CW		1.11×10^{12}				7.66×10^{12}	1.84×10^{4}	40×10^{-6}	14.0 x
LOW CW		1.10×10^{12}				7.59×10^{12}	1.83×10^{4}	40×10^{-6}	14.0 x
LOW CW		1.91×10^{12}				1.31×10^{13}	3.17×10^{4}	40×10^{-6}	14.0 x
HI PULSED		5.55×10^{11}				3.83×10^{12}	9.21×10^{3}	41×10^{-6}	14.3 x
LOW CW		1.11×10^{12}				7.66×10^{12}	1.84×10^{4}	41×10^{-6}	14.3 x
LOW CW		1.21×10^{12}				8.35×10^{12}	2.01×10^{4}	41×10^{-6}	14.3 x
LOW CW		1.64×10^{12}				1.13×10^{13}	2.72×10^{4}	41×10^{-6}	14.3 x
HI PULSED		1.73×10^{12}	2.62×10^{12}	4.70×10^{12}	6.66×10^{12}	1.19×10^{13}	2.87×10^{4}	42×10^{-6}	14.7 x
LOW CW		2.05×10^{12}				1.41×10^{13}			
LOW CW		1.43×10^{12}				9.86×10^{12}	3.40×10^{4}	42×10^{-6}	14.7 x
LOW CW		1.43×10^{12}				9.86×10^{12}	2.37×10^{4}	42×10^{-6}	14.7 x
							2.37×10^{4}	42×10^{-6}	14.7 x
HI PULSED		1.52×10^{12}				1.05×10^{12}			
LOW CW		1.38×10^{12}				9.52×10^{12}	[illegible]	41×10^{-6}	14.3 x
LOW CW		2.14×10^{12}				1.48×10^{13}	2.29×10^{4}	41×10^{-6}	14.3 x
							3.55×10^{4}	41×10^{-6}	14.3 x
LOW CW		1.38×10^{12}				9.52×10^{12}	2.29×10^{4}	41×10^{-6}	14.3 x
HI PULSED		1.55×10^{12}				1.07×10^{13}	2.57×10^{4}	49×10^{-6}	17.1 x
LOW CW		2.12×10^{12}				1.46×10^{13}	3.52×10^{4}	49×10^{-6}	17.1 x
HI PULSED		1.67×10^{12}				1.15×10^{13}	2.77×10^{4}	45×10^{-6}	15.7 x
LOW CW		2.08×10^{12}				1.43×10^{13}	3.45×10^{4}	45×10^{-6}	15.7 x

4

ETRY PROVIL
PONENTS AF

EGRAL DOSE AND DOSE RATE EXPOSURES
BSERVED EFFECTS (SHEET 1)

9	11	12	13	14	15	16	
TED NEUTRON LUX *** CALCULATED TRONS/cm^2)	PULSE WIDTH T_W (SEC.)	REACTOR PERIOD T (SEC.)	R (1/SEC.)	PEAK INCIDENT NEUTRON FLUX RE_n 0.01 (CALCULATED) (NEUTRONS/cm^2 SEC.)	INTEGRATED GAMMA DOSE $D_{\gamma r}$ (RADS)	PEAK INCIDENT GAMMA DOSE $D_{\gamma r}$ (RADS/SEC.)	RADIATION E
24 x 10^{12}	41 x 10^{-6}	14.3 x 10^{-6}	1.75 x 10^{4}	1.27 x 10^{17}	2.15 x 10^{3}	2.28 x 10^{7}	0.04 DB INCREASE IN MON
							0.04 DB DECREASE IN INSE
38 x 10^{12}	41 x 10^{-6}	14.3 x 10^{-6}	1.75 x 10^{4}	1.64 x 10^{17}	2.75 x 10^{3}	2.97 x 10^{7}	0.09 DB INCREASE IN INSE
							0.03 DB INCREASE IN VSWI
31 x 10^{12}	41 x 10^{-6}	14.3 x 10^{-6}	1.75 x 10^{4}	1.63 x 10^{17}	2.60 x 10^{3}	2.94 x 10^{7}	0.23 DB INCREASE IN INSE
14 x 10^{13}	41 x 10^{-6}	14.3 x 10^{-6}	1.75 x 10^{4}	2.00 x 10^{17}	3.40 x 10^{3}	3.50 x 10^{7}	0.06 DB INCREASE IN INSE
54 x 10^{12}	40 x 10^{-6}	14.0 x 10^{-6}	1.79 x 10^{4}	8.13 x 10^{16}	2.59 x 10^{3}	1.46 x 10^{7}	0.05 DB DECREASE IN MON
							0.18 DB INCREASE IN INSE
83 x 10^{12}	40 x 10^{-6}	14.0 x 10^{-6}	1.79 x 10^{4}	1.58 x 10^{17}	3.15 x 10^{3}	2.85 x 10^{7}	0.07 DB INCREASE IN INSE
15 x 10^{13}	40 x 10^{-6}	14.0 x 10^{-6}	1.79 x 10^{4}	2.06 x 10^{17}	3.69 x 10^{3}	3.72 x 10^{7}	0.11 DB INCREASE IN INSE
10 x 10^{13}	40 x 10^{-6}	14.0 x 10^{-6}	1.79 x 10^{4}	1.97 x 10^{17}	4.07 x 10^{3}	3.57 x 10^{7}	0.14 DB INCREASE IN INSE
							0.52 DB INCREASE IN ISOI
26 x 10^{12}	40 x 10^{-6}	14.0 x 10^{-6}	1.79 x 10^{4}	7.63 x 10^{16}	2.75 x 10^{3}	1.37 x 10^{7}	0.05 DB DECREASE IN INSI
66 x 10^{12}	40 x 10^{-6}	14.0 x 10^{-6}	1.79 x 10^{4}	1.37 x 10^{17}	4.15 x 10^{3}	2.47 x 10^{7}	0.07 DB INCREASE IN INSE
							0.02 DB INCREASE IN VSW
59 x 10^{12}	40 x 10^{-6}	14.0 x 10^{-6}	1.79 x 10^{4}	1.36 x 10^{17}	3.41 x 10^{3}	2.46 x 10^{7}	0.26 DB INCREASE IN INSE
31 x 10^{13}	40 x 10^{-6}	14.0 x 10^{-6}	1.79 x 10^{4}	2.35 x 10^{17}	4.41 x 10^{3}	4.26 x 10^{7}	0.21 DB INCREASE IN INSE
							0.50 DB INCREASE IN ISOI
83 x 10^{12}	41 x 10^{-6}	14.3 x 10^{-6}	1.75 x 10^{4}	6.70 x 10^{16}	2.61 x 10^{3}	1.21 x 10^{6}	NO CALIBRATION ON ADA
66 x 10^{12}	41 x 10^{-6}	14.3 x 10^{-6}	1.75 x 10^{4}	1.34 x 10^{17}	4.89 x 10^{3}	2.42 x 10^{7}	0.10 DB INCREASE IN INSE
							0.03 DB INCREASE IN VSW
35 x 10^{12}	41 x 10^{-6}	14.3 x 10^{-6}	1.75 x 10^{4}	1.46 x 10^{17}	3.91 x 10^{3}	2.64 x 10^{7}	0.28 DB INCREASE IN INSE
13 x 10^{13}	41 x 10^{-6}	14.3 x 10^{-6}	1.75 x 10^{4}	1.96 x 10^{17}	4.65 x 10^{3}	3.57 x 10^{7}	0.22 DB INCREASE IN INSE
							0.52 DB INCREASE IN ISOI
19 x 10^{13}	42 x 10^{-6}	14.7 x 10^{-6}	1.70 x 10^{4}	2.02 x 10^{17}	4.19 x 10^{3}	3.66 x 10^{7}	NO CALIBRATION ON MON
41 x 10^{13}							0.09 DB INCREASE IN INSE
86 x 10^{12}	42 x 10^{-6}	14.7 x 10^{-6}	1.70 x 10^{4}	2.40 x 10^{17}	4.15 x 10^{3}	4.34 x 10^{7}	0.16 DB INCREASE IN INSE
86 x 10^{12}	42 x 10^{-6}	14.7 x 10^{-6}	1.70 x 10^{4}	1.66 x 10^{17}	4.40 x 10^{3}	3.02 x 10^{7}	0.07 DB INCREASE IN INSE
	42 x 10^{-6}	14.7 x 10^{-6}	1.70 x 10^{4}	1.68 x 10^{17}	4.15 x 10^{3}	3.02 x 10^{7}	0.11 DB INCREASE IN INSE
05 x 10^{12}	41 x 10^{-6}	14.3 x 10^{-6}	1.75 x 10^{4}	1.84 x 10^{16}	3.80 x 10^{3}	3.48 x 10^{7}	0.10 DB DECREASE IN MO
52 x 10^{12}							0.15 DB INCREASE IN INSE
48 x 10^{13}	41 x 10^{-6}	14.3 x 10^{-6}	1.75 x 10^{4}	1.67 x 10^{17}	3.20 x 10^{3}	3.01 x 10^{7}	0.15 DB INCREASE IN INSE
	41 x 10^{-6}	14.3 x 10^{-6}	1.75 x 10^{4}	2.59 x 10^{17}	4.80 x 10^{3}	4.66 x 10^{7}	0.23 DB INCREASE IN ISOI
52 x 10^{12}							0.06 DB INCREASE IN INSE
	41 x 10^{-6}	14.3 x 10^{-6}	1.75 x 10^{4}	1.67 x 10^{16}	3.20 x 10^{3}	3.01 x 10^{7}	0.08 DB INCREASE IN INSE
07 x 10^{13}	40 x 10^{-6}	17.1 x 10^{-6}	1.46 x 10^{4}	1.56 x 10^{17}	4.35 x 10^{3}	2.81 x 10^{7}	0.10 DB INCREASE IN MON
46 x 10^{13}							0.09 DB INCREASE IN INSE
	40 x 10^{-6}	17.1 x 10^{-6}	1.46 x 10^{4}	2.13 x 10^{17}	3.30 x 10^{3}	3.85 x 10^{7}	0.07 DB INCREASE IN INSE
15 x 10^{13}	39 x 10^{-6}	15.7 x 10^{-6}	1.59 x 10^{4}	1.63 x 10^{17}	3.50 x 10^{3}	3.30 x 10^{7}	0.18 DB IN
							0.15 DB DI
43 x 10^{13}	39 x 10^{-6}	15.7 x 10^{-6}	1.59 x 10^{4}	2.27 x 10^{17}	3.90 x 10^{3}	4.11 x 10^{7}	0.07 DB IN
							2.0 DB INC

5

AND DOSE RATE EXPOSURES

CTS (SHEET 1)

1 LSE TH SEC.)	12 REACTOR PERIOD T (SEC.)	13 R (1 SEC.)	14 PEAK INCIDENT NEUTRON FLUX RE_n 0.01 (CALCULATED) (NEUTRONS/cm^2 SEC.)	15 INTEGRATED GAMMA DOSE D_{GF} (RADS)	16 PEAK INCIDENT GAMMA DOSE D_{GF} (RADS/SEC.)	17 RADIATION EFFECT ON COMPONENTS
10^{-6}	14.3×10^{-6}	1.75×10^{4}	1.27×10^{17}	2.85×10^{3}	2.28×10^{7}	0.04 DB INCREASE IN MONITOR SIGNAL P1 & P2 0.04 DB DECREASE IN INSERTION LOSS P1 & P2
10^{-6}	14.3×10^{-6}	1.75×10^{4}	1.64×10^{17}	3.65×10^{3}	2.97×10^{7}	0.09 DB INCREASE IN INSERTION LOSS 0.03 DB INCREASE IN VSWR SIGNAL
10^{-6}	14.3×10^{-6}	1.75×10^{4}	1.63×10^{17}	3.60×10^{3}	2.94×10^{7}	0.23 DB INCREASE IN INSERTION LOSS
10^{-6}	14.3×10^{-6}	1.75×10^{4}	2.90×10^{17}	6.40×10^{3}	3.50×10^{7}	[illegible] INCREASE IN ISOLATION
10^{-6}	14.0×10^{-6}	1.79×10^{4}	7.13×10^{16}	2.50×10^{3}	1.46×10^{7}	0.05 DB DECREASE IN MONITOR SIGNAL P1 & P2 0.18 DB INCREASE IN INSERTION LOSS P1 & P2
10^{-6}	14.0×10^{-6}	1.79×10^{4}	1.56×10^{17}	5.45×10^{3}	2.85×10^{7}	0.07 DB INCREASE IN INSERTION LOSS
10^{-6}	14.0×10^{-6}	1.79×10^{4}	2.06×10^{17}	7.00×10^{3}	3.72×10^{7}	0.11 DB INCREASE IN INSERTION LOSS
10^{-6}	14.0×10^{-6}	1.79×10^{4}	1.97×10^{17}	6.97×10^{3}	3.57×10^{7}	0.14 DB INCREASE IN INSERTION LOSS 0.52 DB INCREASE IN ISOLATION
10^{-6}	14.0×10^{-6}	1.79×10^{4}	7.68×10^{16}	2.55×10^{3}	1.37×10^{7}	0.05 DB DECREASE IN INSERTION LOSS P1 & P2
10^{-6}	14.0×10^{-6}	1.79×10^{4}	1.47×10^{17}	4.15×10^{3}	2.47×10^{7}	0.07 DB INCREASE IN INSERTION LOSS 0.02 DB INCREASE IN VSWR SIGNAL
10^{-6}	14.0×10^{-6}	1.79×10^{4}	1.46×10^{17}	3.40×10^{3}	2.46×10^{7}	0.26 DB INCREASE IN INSERTION LOSS
10^{-6}	14.0×10^{-6}	1.79×10^{4}	2.37×10^{17}	4.41×10^{3}	4.20×10^{7}	0.21 DB INCREASE IN INSERTION LOSS 0.50 DB INCREASE IN ISOLATION
10^{-6}	14.3×10^{-6}	1.75×10^{4}	7.70×10^{16}	2.60×10^{3}	1.21×10^{7}	NO CALIBRATION ON ADAPTER RETURN SIGNAL
10^{-6}	14.3×10^{-6}	1.75×10^{4}	1.54×10^{17}	4.80×10^{3}	2.42×10^{7}	0.10 DB INCREASE IN INSERTION LOSS 0.03 DB INCREASE IN VSWR SIGNAL
10^{-6}	14.3×10^{-6}	1.75×10^{4}	1.46×10^{17}	3.90×10^{3}	2.64×10^{7}	0.28 DB INCREASE IN INSERTION LOSS
10^{-6}	14.3×10^{-6}	1.75×10^{4}	1.93×10^{17}	4.65×10^{3}	3.57×10^{7}	0.22 DB INCREASE IN INSERTION LOSS 0.52 DB INCREASE IN ISOLATION
10^{-6}	14.7×10^{-6}	1.70×10^{4}	2.02×10^{17}	4.19×10^{3}	3.66×10^{7}	NO CALIBRATION ON MONITOR SIGNAL 0.09 DB INCREASE IN INSERTION LOSS P1 & P2
10^{-6}	14.7×10^{-6}	1.70×10^{4}	2.40×10^{17}	4.15×10^{3}	4.34×10^{7}	0.16 DB INCREASE IN INSERTION LOSS
10^{-6}	14.7×10^{-6}	1.70×10^{4}	1.68×10^{17}	4.40×10^{3}	3.02×10^{7}	0.07 DB INCREASE IN INSERTION LOSS
10^{-6}	14.7×10^{-6}	1.70×10^{4}	1.68×10^{17}	4.15×10^{3}	3.02×10^{7}	0.11 DB INCREASE IN INSERTION LOSS
10^{-6}	14.3×10^{-6}	1.75×10^{4}	1.54×10^{16}	3.80×10^{3}	3.48×10^{7}	0.10 DB DECREASE IN MONITOR SIGNAL P1 & P2 0.15 DB INCREASE IN INSERTION LOSS P1 & P2
10^{-6}	14.3×10^{-6}	1.75×10^{4}	1.67×10^{16}	3.20×10^{3}	3.01×10^{7}	0.15 DB INCREASE IN INSERTION LOSS
10^{-6}	14.3×10^{-6}	1.75×10^{4}	2.59×10^{17}	4.80×10^{3}	4.66×10^{7}	0.23 DB INCREASE IN ISOLATION 0.06 DB INCREASE IN INSERTION LOSS
10^{-6}	14.3×10^{-6}	1.75×10^{4}	1.67×10^{16}	3.20×10^{3}	3.01×10^{7}	0.08 DB INCREASE IN INSERTION LOSS
10^{-6}	17.1×10^{-6}	1.46×10^{4}	1.50×10^{17}	4.31×10^{3}	2.81×10^{7}	0.10 DB INCREASE IN MONITOR SIGNAL P1 & P2 0.09 DB INCREASE IN INSERTION LOSS
10^{-6}	17.1×10^{-6}	1.46×10^{4}	2.13×10^{17}	3.80×10^{3}	3.80×10^{7}	0.07 DB INCREASE IN INSERTION LOSS
10^{-6}	15.7×10^{-6}	1.59×10^{4}	1.63×10^{17}	3.50×10^{3}	3.30×10^{7}	0.16 DB INCREASE IN MONITOR SIGNAL P1 & P2 0.15 DB DECREASE IN INSERTION LOSS P2
10^{-6}	15.7×10^{-6}	1.59×10^{4}	2.27×10^{17}	3.90×10^{3}	4.11×10^{7}	0.07 DB INCREASE IN INSERTION LOSS 2.0 DB INCREASE IN ISOLATION

SYMBOL DEFINITIONS FOR TABLE VI

S	=	DIFFERENCE BETWEEN CENTER OF RADIATION BURST AND CENTER OF P1 (MICROSECONDS)
E_{ns}	=	INTEGRATED NEUTRON FLUX 3.0 Mev (NEUTRONS cm^2)
$E_n 1.5$	=	INTEGRAL NEUTRON FLUX 1.5 Mev (NEUTRONS cm^2)
	=	$\frac{E_{ns}}{.145}$
$E_n 0.6$	=	INTEGRAL NEUTRON FLUX 0.7 Mev (NEUTRONS cm^2)
$E_n 0.01$	=	INTEGRAL NEUTRON FLUX 0.01 Mev (NEUTRONS cm^2)
D_n	=	FIRST COLLISION TISSUE DOSE OF NEUTRONS (RADS)
	=	$1.66 \times 10^{-8} E_{ns}$ WHERE 1.66×10^{-8} IS AN EMPIRICAL NUMBER
T_w	=	RADIATION PULSE WIDTH AT ONE-HALF MAXIMUM OBTAINED FROM SPRF PHOTOGRAPH (SECONDS)
T	=	REACTOR PERIOD = $\frac{1}{2.86} T_w$ WHERE $\frac{1}{2.86}$ IS AN EMPIRICAL NUMBER (SEC.)
R	=	RATIO OF PEAK NEUTRON FISSION RATE TO THE TOTAL NEUTRON FISSIONS $\frac{1}{4T}$
D_g	=	INTEGRATED GAMMA DOSE (RADS)
D_{gr}	=	PEAK GAMMA DOSE RATE (RADS SEC.)

NOTES:

* Power level delivered to the component under test. { Hi pulsed ~ 5kw / Low cw ~ 100 milliwatts

** Positive sign indicates the center of the radiation burst was ahead of the center of P1.

*** $E_n 0.01$ was calculated assuming E_{ns} 0.145 $E_n 0.01$.

LE VI

ADIATION BURST AND

(NEUTRONS cm^2)

EUTRONS cm^2)

EUTRONS cm^2)

NEUTRONS cm^2)

UTRONS (RADS)

AN EMPIRICAL NUMBER

LF MAXIMUM OBTAINED

IS AN EMPIRICAL

2. 86

TE TO THE TOTAL NEUTRON

1 BURST NUMBER	2 COMPONENT EXPOSED	3 POWER LEVEL *	4 S** (MICROSECONDS)	5 INTEGRATED NEUTRON FLUX E_{ns} (NEUTRONS cm^2)
9	COAXIAL DUPLEXER	HI PULSED	- 5	2.09 x 10^{12}
	W/G CIRCULATOR	LOW CW		1.45 x 10^{12}
		LOW CW		1.03 x 10^{12}
	ALUMINUM W/G (AIR FILLED)	LOW CW		1.49 x 10^{12}
10	COAXIAL DUPLEXER	HI PULSED	+15	2.79 x 10^{12}
	W/G CIRCULATOR	LOW CW		1.59 x 10^{12}
	W/G DUPLEXER	LOW CW		1.20 x 10^{12}
	ALUMINUM W/G (AIR FILLED)	LOW CW		1.89 x 10^{12}
11	W/G CIRCULATOR	HI PULSED	- 5	1.34 x 10^{12}
	W/G DUPLEXER	LOW CW		1.16 x 10^{12}
12	W/G CIRCULATOR	HI PULSED	- 3	1.39 x 10^{12}
	W/G DUPLEXER	LOW CW		1.35 x 10^{12}
	COAXIAL LIMITER	LOW CW		1.21 x 10^{12}
13	W/G CIRCULATOR	HI PULSED	-10	1.40 x 10^{12}
14	W/G CIRCULATOR	LOW CW	-42	1.19 x 10^{12}
15	W/G CIRCULATOR	LOW CW	-30	[illegible] x 10^{12}
	COAXIAL LIMITER	LOW CW		[illegible] x 10^{12}
16	W/G CIRCULATOR	LOW CW	-15	[illegible] x 10^{12}
17	W/G CIRCULATOR	LOW CW	–	[illegible] x 10^{12}
	ALUMINUM W/G (HI DENSITY POLY)	LOW CW		[illegible] x 10^{12}
18	COAXIAL CI[illegible]ULATOR	HI PULSED	0	[illegible] x 10^{12}
	COAXIAL LIMITER	LOW CW		1.37 x 10^{12}
	COAXIAL CIRCULATOR	LOW CW		1.18 x 10^{12}
	ALUMINUM W/G (HI DENSITY POLY)	LOW CW		1.52 x 10^{12}

Hi pulsed 5kw

ent under test.

Low cw 100 milliwatts

the radiation burst was ahead

2

TABLE VI. NEUTRON AND γ-RAY DOSIMETRY PROVIDING INTEGRAL DOSE AND DO
TO THE MICROWAVE COMPONENTS AND THE OBSERVED EFFECTS

3	4	5	6	7	8	9	10	11	12
POWER LEVEL *	** (MICROSECOND)	INTEGRATED NEUTRON FLUX E_{ns} (NEUTRONS cm^2)	INTEGRATED NEUTRON FLUX (BORON BALL) (NEUTRONS cm^2)			INTEGRATED NEUTRON FLUX *** E_n 0.01 (CALCULATED) (NEUTRONS cm^2)	NEUTRON TISSUE DOSE D_n (RADS)	PULSE WIDTH T_w (SEC.)	REACTOR PERIOD T (SEC)
			E_n 1.5	E_n 0.6	E_n 0.01				
HI PULSED		2.09×10^{12}				1.44×10^{13}	3.47×10^4	50×10^{-6}	17.5×1
LOW CW		1.45×10^{12}				1.00×10^{13}	2.41×10^4	50×10^{-6}	17.5×1
LOW CW		1.03×10^{12}				7.10×10^{12}	1.71×10^4	50×10^{-6}	17.5×1
LOW CW		1.49×10^{12}				1.03×10^{13}	2.47×10^4	50×10^{-6}	17.5×1
HI PULSED		2.79×10^{12}	1.75×10^{12}	3.76×10^{12}	4.91×10^{12}	1.92×10^{13}	4.63×10^4	46×10^{-6}	$16.1 \times$
LOW CW		1.59×10^{12}				1.10×10^{13}	2.64×10^4	46×10^{-6}	$16.1 \times$
LOW CW		1.20×10^{12}				8.26×10^{12}	1.99×10^4	46×10^{-6}	[illegible]
LOW CW		1.89×10^{12}				1.30×10^{13}	3.13×10^4	46×10^{-6}	[illegible]
HI PULSED		1.34×10^{12}	1.67×10^{12}	3.16×10^{12}	4.55×10^{12}	9.24×10^{12}	2.22×10^4	50×10^{-6}	$17.5 \times$
LOW CW		1.16×10^{12}				8.00×10^{12}	1.93×10^4	50×10^{-6}	$17.5 \times$
HI PULSED		1.39×10^{12}				9.59×10^{12}	2.31×10^4	50×10^{-6}	$17.5 \times$
LOW CW		1.35×10^{12}				9.31×10^{12}	2.24×10^4	50×10^{-6}	$17.5 \times$
LOW CW		1.21×10^{12}				8.34×10^{12}	2.01×10^4	50×10^{-6}	$17.5 \times$
HI PULSED		1.40×10^{12}				9.66×10^{12}	2.32×10^4	50×10^{-6}	$17.5 \times$
LOW CW		1.19×10^{12}				8.21×10^{12}	1.98×10^4	60×10^{-6}	$21.0 \times$
LOW CW		1.51×10^{12}				1.04×10^{13}	2.51×10^4	50×10^{-6}	$17.5 \times$
LOW CW		1.50×10^{12}				1.0×10^{13}	2.4×10^4	50×10^{-6}	$17.5 \times$
LOW CW		1.33×10^{12}	3.02×10^{12}	5.54×10^{12}	8.25×10^{12}	9.17×10^{12}	2.21×10^4	52×10^{-6}	$18.2 \times$
LOW CW		1.49×10^{12}				1.03×10^{13}	2.47×10^4		
LOW CW		1.76×10^{12}				1.21×10^{13}	2.92×10^4		
HI PULSED		1.18×10^{12}	2.85×10^{12}	5.34×10^{12}	7.77×10^{12}	8.14×10^{12}	1.96×10^4	50×10^{-6}	$17.5 \times$
LOW CW		1.37×10^{12}				9.45×10^{12}	2.27×10^4	50×10^{-6}	$17.5 \times$
LOW CW		1.18×10^{12}				8.14×10^{12}	1.96×10^4	50×10^{-6}	$17.5 \times$
LOW CW		1.52×10^{12}				1.05×10^{13}	2.52×10^4	50×10^{-6}	$17.5 \times$

3

DOSIMETRY PRO ... **NTEGRAL DOSE AND DOSE RATE EXPOSURES**
WAVE COMPONE ... **HE OBSERVED EFFECTS (SHEET 2)**

9 ATED NEUTRON LUX *** (CALCULATED) TRONS, cm^2)	11 PULSE WIDTH P_w (SEC.)	12 REACTOR PERIOD T (SEC.)	13 R (1/SEC.)	14 PEAK INCIDENT NEUTRON FLUX ϕE_n 0.01 (CALCULATED (NEUTRONS/cm^2 SEC.)	15 INTEGRATED GAMMA DOSE Dgr (RADS)	16 PEAK INCIDENT GAMMA DOSE Dgr (RADS/SEC.)	RADIATION
$.44 \times 10^{13}$	50×10^{-6}	17.5×10^{-6}	1.43×10^{4}	2.06×10^{17}	4.05×10^{3}	3.72×10^{7}	0.15 DB INCREASE IN MO 0.06 DB DECREASE IN INS
$.00 \times 10^{13}$	0×10^{-6}	17.5×10^{-6}	1.43×10^{4}	1.43×10^{7}	3.25×10^{3}	2.59×10^{7}	0.12 DB INCREASE IN INS NO CALIBRATION ON VSW
$.10 \times 10^{12}$	0×10^{-6}	17.5×10^{-6}	1.43×10^{4}	2.45×10^{16}	2.65×10^{3}	1.83×10^{7}	
$.03 \times 10^{13}$	0×10^{-6}	17.5×10^{-6}	1.43×10^{4}	1.47×10^{17}	3.45×10^{3}	2.65×10^{7}	0.36 DB INCREASE IN INS
$.92 \times 10^{13}$	0×10^{-6}	16.1×10^{-6}	1.55×10^{4}	2.98×10^{17}	5.60×10^{3}	5.38×10^{7}	0.17 DB INCREASE IN MO 1.12 DB INCREASE IN INS
$.10 \times 10^{13}$	0×10^{-6}	16.1×10^{-6}	1.55×10^{4}	1.71×10^{17}	3.25×10^{3}	3.07×10^{7}	0.15 DB INCREASE IN INS
$.00 \times 10^{12}$	0×10^{-6}	16.1×10^{-6}	1.55×10^{4}	1.28×10^{17}	2.95×10^{3}	2.13×10^{7}	.19 DB INCREASE IN INS
$.00 \times 10^{13}$	0×10^{-6}	16.1×10^{-6}	1.55×10^{4}	2.02×10^{17}	3.50×10^{3}	2.96×10^{7}	.15 DB INCREASE IN INS
$.24 \times 10^{12}$	0×10^{-6}	17.5×10^{-6}	1.43×10^{4}	1.32×10^{17}	1.85×10^{3}	2.38×10^{7}	0.04 DB INCREASE IN MO 0.10 DB DECREASE IN P1
$.00 \times 10^{12}$	0×10^{-6}	17.5×10^{-6}	1.43×10^{4}	1.14×10^{17}	2.90×10^{3}	2.07×10^{7}	0.16 DB INCREASE IN INS
$.59 \times 10^{12}$	0×10^{-6}	17.5×10^{-6}	1.43×10^{4}	1.37×10^{17}	2.95×10^{3}	2.48×10^{7}	0.03 DB INCREASE IN MO 0.11 DB INCREASE IN INS
$.31 \times 10^{12}$	0×10^{-6}	17.5×10^{-6}	1.43×10^{4}	1.33×10^{17}	1.90×10^{3}	2.40×10^{7}	0.24 DB INCREASE IN INS
$.34 \times 10^{12}$	0×10^{-6}	17.5×10^{-6}	1.43×10^{4}	1.19×10^{17}	2.30×10^{3}	2.16×10^{7}	0.02 DB INCREASE IN VSW
$.66 \times 10^{12}$	0×10^{-6}	17.5×10^{-6}	1.43×10^{4}	1.38×10^{17}	3.15×10^{3}	2.49×10^{7}	0.02 DB INCREASE P1, 0. 0.07 DB INCREASE INSER
$.21 \times 10^{12}$	$\times 10^{-6}$	21.0×10^{-6}	1.19×10^{4}	9.77×10^{16}	2.55×10^{3}	1.77×10^{7}	0.09 DB INCREASE IN INS
$.04 \times 10^{13}$	0×10^{-6}	17.5×10^{-6}	1.43×10^{4}	1.49×10^{17}	3.65×10^{3}	2.69×10^{7}	0.10 DB INCREASE IN INS
$.0 \times 10^{13}$	0×10^{-6}	17.5×10^{-6}	1.43×10^{4}	1.49×10^{17}	3.6×10^{3}	2.6×10^{7}	10 DB INCREASE IN SIGNA
$.17 \times 10^{12}$	$.2 \times 10^{-6}$	18.2×10^{-6}	1.37×10^{4}	1.26×10^{17}	2.80×10^{3}	2.27×10^{7}	0.11 DB INCREASE IN INS
$.03 \times 10^{13}$					3.15×10^{3}		0.06 DB INCREASE IN MO 0.15 DB INCREASE IN INS
$.21 \times 10^{13}$					2.40×10^{3}		0.21 DB INCREASE IN INS
$.14 \times 10^{12}$	0×10^{-6}	17.5×10^{-6}	1.43×10^{4}	1.16×10^{17}	2.85×10^{3}	2.10×10^{7}	0.22 DB DECREASE IN MO 0.08 DB DECREASE IN INS
$.45 \times 10^{12}$	0×10^{-6}	17.5×10^{-6}	1.43×10^{4}	1.35×10^{17}	2.85×10^{3}	2.44×10^{7}	0.09 DB INCREASE IN INS
$.14 \times 10^{12}$	0×10^{-6}	17.5×10^{-6}	1.43×10^{4}	1.16×10^{17}	2.85×10^{3}	2.10×10^{7}	NO CALIBRATION VSWR S
$.05 \times 10^{13}$	0×10^{-6}	17.5×10^{-6}	1.43×10^{4}	1.50×10^{17}	2.00×10^{3}	2.70×10^{7}	0.20 DB INCREASE IN INS

4

DOSE RATE EXPOSURES

TS (SHEET 2)

12 CTOR RIOD SEC.)	13 R (1 SEC.)	14 PEAK INCIDENT NEUTRON FLUX RE_n 0.01 (CALCULATED (NEUTRONS cm^2 SEC.)	15 INTEGRATED GAMMA DOSE D_{gr} (RADS)	16 PEAK INCIDENT GAMMA DOSE D_{gr} (RADS SEC.)	17 RADIATION EFFECT ON COMPONENTS
x 10^{-6}	1.43 x 10^4	2.06 x 10^{17}	4.05 x 10^3	3.72 x 10^7	0.15 DB INCREASE IN MONITOR SIGNAL P1 & P2 0.06 DB DECREASE IN INSERTION LOSS P2
x 10^{-6}	1.43 x 10^4	1.43 x 10^7	3.25 x 10^3	2.59 x 10^7	0.12 DB INCREASE IN INSERTION LOSS NO CALIBRATION ON VSWR SIGNAL
x 10^{-6}	1.43 x 10^4	2.45 x 10^{16}	2.65 x 10^3	1.83 x 10^7	
x 10^{-6}	1.43 x 10^4	1.47 x 10^{17}	3.45 x 10^3	2.65 x 10^7	0.36 DB INCREASE IN INSERTION LOSS
x 10^{-6}	1.55 x 10^4	2.98 x 10^{17}	5.60 x 10^3	5.38 x 10^7	0.17 DB INCREASE IN MONITOR SIGNAL P1 & P2 1.12 DB INCREASE IN INSERTION LOSS P1 & P2
x 10^{-6}	1.55 x 10^4	1.71 x 10^{17}	3.25 x 10^3	3.07 x 10^7	0.15 DB INCREASE IN INSERTION LOSS
[illegible]	[illegible]	[illegible]	2.95 x 10^3	[illegible]	[illegible] DB INCREASE IN INSERTION LOSS
[illegible]	[illegible]	[illegible]	3.50 x 10^3	[illegible]	[illegible] DB INCREASE IN INSERTION LOSS
x 10^{-6}	1.43 x 10^4	1.32 x 10^{17}	1.85 x 10^3	2.38 x 10^7	0.04 DB INCREASE IN MONITOR SIGNAL P1 & P2 0.10 DB DECREASE IN P1, 0.02 DB DECREASE P2 INSERTION LOSS
x 10^{-6}	1.43 x 10^4	1.14 x 10^{17}	2.90 x 10^3	2.07 x 10^7	0.16 DB INCREASE IN INSERTION LOSS
x 10^{-6}	1.43 x 10^4	1.37 x 10^{17}	2.95 x 10^3	2.48 x 10^7	0.03 DB INCREASE IN MONITOR SIGNAL P1 & P2 0.11 DB INCREASE IN INSERTION LOSS P1 & P2
x 10^{-6}	1.43 x 10^4	1.33 x 10^{17}	1.90 x 10^3	2.40 x 10^7	0.24 DB INCREASE IN INSERTION LOSS
x 10^{-6}	1.43 x 10^4	1.19 x 10^{17}	2.30 x 10^3	2.16 x 10^7	0.02 DB INCREASE IN VSWR SIGNAL
x 10^{-6}	1.43 x 10^4	1.38 x 10^{17}	3.15 x 10^3	2.49 x 10^7	0.02 DB INCREASE P1, 0.02 DB DECREASE P2 MONITOR SIGNAL 0.07 DB INCREASE INSERTION LOSS P1
x 10^{-6}	1.19 x 10^4	9.77 x 10^{16}	2.55 x 10^3	1.77 x 10^7	0.09 DB INCREASE IN INSERTION LOSS
x 10^{-6}	1.43 x 10^4	1.49 x 10^{17}	3.65 x 10^3	2.69 x 10^7	0.10 DB INCREASE IN INSERTION LOSS
x 10^{-6}	1.43 x 10^4	1.49 x 10^{17}	3.6 x 10^3	2.6 x 10^7	10 DB INCREASE IN SIGNAL LEVEL FROM OUTPUT PORT
x 10^{-6}	1.37 x 10^4	1.26 x 10^{17}	2.80 x 10^3	2.27 x 10^7	0.11 DB INCREASE IN INSERTION LOSS
			3.15 x 10^3		0.06 DB INCREASE IN MONITOR SIGNAL 0.15 DB INCREASE IN INSERTION LOSS
			2.40 x 10^3		0.21 DB INCREASE IN INSERTION LOSS
x 10^{-6}	1.43 x 10^4	1.16 x 10^{17}	2.85 x 10^3	2.10 x 10^7	0.22 DB DECREASE IN MONITOR SIGNAL P1 & P2 0.08 DB DECREASE IN INSERTION LOSS P1 & P2
x 10^{-6}	1.43 x 10^4	1.35 x 10^{17}	2.85 x 10^3	2.44 x 10^7	0.09 DB INCREASE IN INSERTION LOSS
x 10^{-6}	1.43 x 10^4	1.16 x 10^{17}	2.85 x 10^3	2.10 x 10^7	NO CALIBRATION VSWR SIGNAL
x 10^{-6}	1.43 x 10^4	1.50 x 10^{17}	2.00 x 10^3	2.70 x 10^7	0.20 DB INCREASE IN INSERTION LOSS

5

5. CONCLUSIONS

The following conclusions are based on the operation of C-band microwave components at power levels of 100 milliwatts (low power) and 5 kilowatts (high power) at a frequency of 5.6 Gc and in a radiation environment of the content and duration of that produced during a burst at the SPRF. The radiation effects on the operating characteristics of the components are the following:

5.1 WAVEGUIDE TO COAXIAL ADAPTERS

The average transient decrease in the signal level passing through the adapters using rexolite beads was approximately 0.1db at low rf power. Under the same operating conditions, the average transient decrease in the signal level passing through the adapters using polyethylene beads was less than 0.2 db or approximately twice that of the rexolite beads. Transient effects observed at high rf pulsed power were of comparable magnitude.

5.2. ALUMINUM WAVEGUIDE SECTIONS

Air ionization effects in waveguide have been noted in previous experiments Tests performed during this interim using carefully selected adapters (Rexolite beads) are consistent with the previous conclusions. Solid dielectric inserts reduce the ionization effects and thus the transient increase in insertion loss per foot; however these inserts increase the static insertion loss of the waveguide by approximately an order of magnitude.

5.3. COAXIAL ISOLATOR

The radiation effects observed were less than 0.1 db. The device seems to be fully acceptable for use in a radiation environment.

5.4 COAXIAL CIRCULATOR

The high and low power transient effects observed for this device are less than 0.05 db. This device seems to be fully operational in a transient radiation environment.

5.5 COAXIAL LIMITER

The transient radiation effects observed for this device at low r-f power are less than 0.1 db and are thus acceptably low. At high power the signal level out of the limiter increases by approximately 10 db. The basic source of this effect is

believed to be associated with the teflon bead used for the single crystal sphere holder and cross strip spacer. Some redesign and additional tests on the device seem required to produce a fully radiation resistance gyromagnetic coupling limiter.

5.6 COAXIAL DUPLEXER

This device composed of the coaxial Y-junction circulator and the coaxial limiter seem to be acceptable for use in a radiation environment. The observed average transient radiation effects were less than 0.2 db. The isolation provided by the circulator seems to reduce the rf power reaching the limiter to a magnitude below that producing the adverse effects observed in the tests of the limiter alone. This of course, depends on the application and system environment of the duplexer.

5.7 WAVEGUIDE JUNCTION CIRCULATOR

The average transient radiation effects observed for this component at low or high power are less than 0.15 db. The operation of this device seems acceptable for utilization in a radiation environment.

5.8 WAVEGUIDE DIFFERENTIAL PHASE SHIFT DUPLEXER

The average transient radiation effects observed for this component at low or high power are less than 0.3 db. A large portion of this observed effect is possibly associated with the waveguide-to-coax adapters required to perform the tests. The actual radiation effects in the duplexer proper is probably near 0.1 db.

5.9 MAGNETRON AND FREQUENCY METER

Tests on the bare magnetron operating in the pulse radiation environment produced no deterioration in the pulse shape or magnitude. Previous experiments which included the pulse transformer and associated circuitry produced results showing large decreases in output power during and just after the radiation burst. These effects are attributed to the pulse transformer and circuitry supplementary to the magnetron. The magnetron itself apparently operates without deterioration during the radiation burst.

The observed signals from the frequency meter tests could not be fully analyzed. However, the characteristics of the transmission cavities apparently were altered during the burst producing large excursions in the output signal.

5.10 GENERAL

In general, the effects of the radiation experimental tests during this period agree well with those reported for previous periods. With the exception of the coaxial

limiter, the observed effects at high r-f power levels (5 Kw) agree well with those observed at low cw power.

The operating characteristics of all the ferrite duplexing components tested in the pulsed radiation environment (with the possible exception of the coaxial gyromagnetic coupling limiter) are not altered severely. Each component would be acceptable for utilization toward radiation resistant or hardened microwave system.

The significance of these conclusions to the microwave equipment designer is as follows:

> The gyromagnetic coupling limiters can not be expected to retain their full limiting characteristic when exposed to pulsed radiation and high rf power. In critical power limiting situations, some degree of radiation resistant development will be needed for the limiter to perform properly. All of the other components tested seem fully acceptable for utilization in radiation resistant microwave equipment.

The significance of these conclusions to the microwave tube designers is the following:

> The magnetron (MA-220) and pulse transformer exhibited large transient effects during the radiation burst and recovery time (lingering effects) are long (much longer than 150 microseconds). The magnetron itself exhibits radiation resistant characteristics. Radiation effects in the pulse transformer and associated driver circuitry produce the observed deteriorating effects.

The significance of these conclusions to individuals engaged in the study of radiation damage mechanisms is the following:

> Ionization produced by gamma rays and the resultant electrons is the most prominent radiation damage mechanism observed in the studies of transient radiation effects on microwave duplexing equipment.

6. REFERENCES

1. Harrison, G. R. and Scheiwe, J. P., "Study of Pulsed Radiation Effects on Microwave Ferrite Duplexers," Report No. 1 Contract No. DA 36-039-SC-89113, First Quarterly Report, Sperry Microwave Electronics.

2. Harrison, G. R. and Scheiwe, J. P., "Study of Pulsed Radiation Effects on Microwave Ferrite Duplexers," Report No. 2 Contract No. DA 36-039-SC-89113, Second Quarterly Report, Sperry Microwave Electronics Co.

3. Harrison, G. R. and Scheiwe, J. P., "Study of Pulsed Radiation Effects on Microwave Ferrite Duplexers," Report No. 3 Contract No. DA-36-039-SC-89113, Third Quarterly Report, Sperry Microwave Electronics Co.

4. Scheiwe, J. P. and Harrison, G. R., "Study of Pulsed Radiation Effects on Microwave Ferrite Duplexers," Report No. 4 Contract No. DA 36-039-SC-89113, Fourth Quarterly Report, Sperry Microwave Electronics Co.

5. Hart, J. A., Harrison, G. R., and Greenwood, R. E., "Study of Pulsed Radiation Effects on Microwave Ferrite Duplexers," Report No. 5 Contract No. DA 36-039-SC-89113, Fifth Quarterly Report, Sperry Microwave Electronics Co.

6. Hart, J. A., Harrison, G. R., and Greenwood, R. E., "Study of Pulsed Radiation Effects on Microwave Ferrite Duplexers," Report No. 6 Contract No. DA 36-039-SC-89113, Sixth Quarterly Report, Sperry Microwave Electronics Co.

7. Private communication with P. D. O'Brien.

8. Private communication with L. L. Flores.

9. Plankis, E. P., "Radiation Effects on Microwave Devices," Report No. 3 Contract No. DA-36-039-SC-87253, Third Quarterly Progress Report, General Electric Co., Power Tube Department, p 69 and p 73.

7. PROGRAM FOR NEXT INTERVAL

(1 MARCH 1964 TO 31 JULY 1964)

The data collected during the entire program will be further analyzed and integrated. A thorough analysis and interpretation of the results of the program will be formalized leading to the preparation of the final report.

8. IDENTIFICATION OF PERSONNEL

During the sixth quarter (1 November to 29 February), 567 engineering manhours were devoted to the contract by the personnel listed below.

Biographies of all personnel have appeared in previous reports submitted on the program.

B. J. Duncan	9 hours
E. W. Matthews	27 hours
G. R. Harrison	95 hours
R. E. Greenwood	112 hours
J. A. Hart	281 hours
D. B. Swartz	43 hours

Distribution List

Address	No. of Copies
Defense Documentation Center ATTN: TISIA Cameron Stn., Bldg. 5 Alexandria, Va. 22314	20
Advisory Group on Electron Devices 346 Broadway, 8th Floor New York, N.Y. 10013	3
OASD (R&E), Rm. 3E ATTN: Technical Library The Pentagon Washington, D.C. 20301	1
Chief of Research & Development OCS, Dept. of the Army Washington 25, D.C.	1
Commander, U. S. Army Research Office (DURHAM) Box CM-DUKE Station Durham, N.C.	1
Chief, U.S. Army Security Agency Arlington Hall Station Arlington 12, Va.	2
Deputy President U. S. Army Security Agency Board Arlington Hall Station Arlington 12, Va.	1
Commanding General U. S. Army Combat Dev. Command ATTN: CDCMR-E Ft. Belvoir, Va. 22060	1
Director, Monmouth Office U. S. Army Combat Developments Command Communications-Electronics Agency Ft. Monmouth, N.J. 07703	1
Commanding Officer U. S. Army Combat Development Command Communications-Electronics Agency Ft. Huachuca, Ariz. 85613	1

Address	No. of copies
Commanding Officer Engineering R&D Labs ATTN: STINFO Branch Ft. Belvair, Virginia 22060	2
Commanding Officer U.S. Army Missile Command ATTN: Technical Library Redstone Arsenal, Ala	1
Commanding Officer Harry Diamond Laboratories Connecticut Avenue and Van Ness St., N.W. Washington, D.C. 20438	1
Commanding General U.S. Army Materiel Command ATTN: R&D Directorate Washington, D.C. 20315	1
Commanding General U.S. Army Electronics Command ATTN: AMSEL-AD Ft. Monmouth, N.J. 07703	1
Commanding Officer U.S. Army Electronics Research & Development Laboratories ATTN: Director of Research Ft. Monmouth, N.J. 07703	1
Commanding Officer U.S. Army Electronics R&D Laboratories ATTN: AMSEL-RD-ADO-RHA Ft. Monmouth, N.J. 07703	1
Commanding Officer (Record Copy) U.S. Army Electronics Research & Development Laboratories ATTN: AMSEL-RD-PRT Ft. Monmouth, N.J. 07703	
Commanding Officer U.S. Army Electronics Research & Development Laboratories ATTN: Logistics Division (For AMSEL-RD-PRT, Proj. Engineer) Ft. Monmouth, N.J. 07703	1

Address	No. of copies
Commanding Officer U.S. Army Electronics R&D Laboratories ATTN: AMSEL-RD-PR (Contracts) -PR (Tech Staff) -PRG (Mr. Zinn) -PRM (Mr. Hersh) Ft. Monmouth, N.J. 07703	1 1 1 1
Commanding Officer U.S. Army Electronics Research & Development Laboratories ATTN: Technical Documents Center Ft. Monmouth, N.J. 07703	1
USAELRDL Liaison Office Rome Air Development Center ATTN: RAOL Griffiss AFB, N.Y. 13442	1
Commanding Officer U.S. Army Electronics Materiel Agency ATTN: SELMA-R2a 225 South 18th. Street Philadelphia, Pa. 19103	1
Commanding Officer U.S. Army Electronics Materiel Support Agency ATTN: SELMS-ADJ Ft. Monmouth, N.J. 07703	1
Commanding Officer U.S. Army Electronics Research Unit P.O. Box 205 Mountain View, California	1
Director, U.S. Naval Research Laboratory ATTN: Code 2027 Washington, D.C. 20390	1
Chief, Bureau of Ships Dept. of the Navy ATTN: Code 681A-1 Washington 25, D.C.	1
Commanding Officer and Director U.S. Navy Electronics Laboratory San Diego 52, California	1

Address	No. of copies
Marine Corps Liaison Office U.S. Army Electronics Research & Development Laboratories Ft. Monmouth, N.J. 07703	1
Commander Aeronautical Systems Division ATTN: ASNXRR Wright-Patterson Air Force Base, Ohio 45433	1
Hq., Aeronautical Systems Division ATTN: ASRNE Wright-Patterson Air Force Base, Ohio 45433	1
Commander, Rome Air Development Center ATTN: RAALD Griffiss Air Force Base, N.Y. 13442	1
Commander Air Force Cambridge Research Laboratories ATTN: CRXL-R L.G. Hanscom Field Bedford, Mass 01731	1
Commander, Air Force Command and Control Development Division ATTN: CRZC L.G. Hanscom Field Bedford, Mass. 01731	1
HQ., Electronic Systems Division ATTN: ESTI L. G. Hanscom Field Bedford, Mass. 01731	1
AFSC Scientific/Technical Liaison Office USAELRDL Ft. Monmouth, N.J. 07703	1
AFC Scientific/Technical Liaison Office U.S. Naval Air Development Center Johnsville, Pa. 18974	1
Commanding Officer U.S. Army Electronics R&D Activity ATTN: SELWS-A White Sands, N. Mexico 88002	1

Address	No. of copies
Radiation Effects Information Center Battelle Memorial Institute 505 King Avenue Columbus, Ohio ATTN: Mr. D.C. Jones	1
Chief Defense Atomic Support Agency ATTN: DASARA-4 Washington, D.C. 20301	1
Director Defense Atomic Support Agency ATTN: Document Library Branch Washington, D.C. 20301	1
Commander Field Command Defense Atomic Support Agency ATTN: FCWT ATTN: SPRF Coordinator Sandia Base Albuquerque, N. Mexico 87115	1 1
Director Defense Intelligence Agency ATTN: DIAAP-1K2 Washington, D.C. 22212	1
Director Advanced Research Projects Agency Washington, D.C. 20301 ATTN: Lt. Col W.H. Innes ATTN: Maj G.L. Sherwood	1 1
Chief of Research and Development Department of Army Washington, D.C. 20301 ATTN: Lt. Col D. Baker, Atomics Division	1
Commanding General U.S. Army Materiel Command ATTN: AMCRD-DE-N Washington, D.C. 20315	1
HQ Army Materiel Command Development Div., Nuclear Br. AMCRD-DN ATTN: Mr. Stulman Washington, D.C. 20315	1

Address	No of copies
Commanding Officer U.S. Army Office of Special Weapons Development ATTN: Major Doerflinger Fort Bliss, Texas	1
Commanding Officer Harry Diamond Laboratories ATTN: Chief, Nuclear Vulnerability Branch (230) Washington, D.C. 20438	1
Commanding General U.S. Army Munitions Command Picatinny Arsenal Dover, N.J. 07801 Attn: Mr. R.K. Benson	1
Commanding Officer U.S. Army Electronics Laboratories ATTN: AMSEL-RD-PE (Dr. E. Both) ATTN: AMSEL-RD-P (B. Louis) Fort Monmouth, N.J. 07703	 1 1
Chief of Naval Research Navy Department ATTN: Codes 418 and 427 Washington 25, D.C.	1
Chief, Bureau of Ships Navy Department ATTN: Code 362B Washington, D.C. 20360	1
Chief of Naval Operations Navy Department ATTN: OP-754 Washington, D.C. 20350	1
Chief, Bureau of Naval Weapons Navy Department ATTN: RMGA-8 and RRNU Washington, D.C. 20360	1
CO, Naval Weapons Evaluation Facility ATTN: Code 3434 Kirtland Air Force Base N. Mexico 87117	1

Address	No. of copies
Commander Naval Ordnance Laboratory, White Oak ATTN: Mr. Grantham Silver Spring, Maryland 20390	1
Commanding Officer Naval Ordnance Laboratory ATTN: Dr. Bryant Corona, California 91720	1
Commander U.S. Naval Applied Science Lab. U.S. Naval Base Brooklyn 1, N.Y	1
Commanding Officer Naval Air Development Center Johnsville, Pa. 18974	1
Commanding Officer Naval Aviation Materiel Center Philadelphia, Pa.	1
Commanding Officer and Director U.S. Naval Radiological Defense Laboratory San Francisco 24, California	1
HQ. USAF ATTN: AFDRP-S ATTN: AFTAC ATTN: AFRDC/NE Washington, D.C. 20330	1 1 1
ADC (ADOOP) Ent AFB Colo. 80912	1
AFSC(SCR, DCS/R&E) Andrews AFB Md 20331	1
HQ. AFWL Kirtland AFB, N. Mexico 87117 ATTN: (WLDN) (WLRPA) (WLL)	1 1 1

[redacted]

Address	No of copies
AFGC (PGAPI) Eglin AFB Fla. 32542	1
BSD (BSRGA) Norton AFB, Calif. 92409	1
FTD (TD-BI) Wright-Patterson AFB, Ohio 45433	1
RADC ATTN: RAS Griffiss AFB NY 13442 ATTN: RASSM-1	1 1
HQ R&T Div Bolling AFB Washington, D.C. 20332	1
SAC (DPLLC) and (OAWS) Offutt AFB Nebr. 68113	1
SSD (SSTS) and (SSZME) at Unit Post Office Los Angeles 45, Calif.	1
TAC (TPL-RQD-M) Langley AFB Ba. 23365	1
Admiral Corporation 3800 Cortland Street Chicago 47, Ill. ATTN: Mr. R. Whitner	1
The Johns Hopkins University Applied Physics Laboratory 8621 Georgia Avenue Silver Spring, Md ATTN: Mr. Robert Freiberg (Via BuWeps. Rep. APL/JHU)	1
ARINC Research Corporation 1700 K Street N.W. Washington, D.C. 20006 ATTN: Mr. Wm. H. VonAlven	1
Bell Telephone Labs., Inc. 463 West Street New York, N.Y	1
The Boeing Company, Aerospace Division 7755 E. Marginal Way Seattle 8, Washington ATTN: Dr. Glenn Keister	1

Address	No. of copies
Brookhaven National Laboratory Tech Info Div., Documents Group Upton, Long Island, N.Y. 11973 ATTN: Dr. G.H. Vineyard	1
Burroughs Corporation Central Avenue & Route 202 Paoli, Pa. ATTN: Mr. Alton L. Long	1
General Atomic Div. P.O. Box S. Old San Diego Sts. San Diego, Calif. ATTN: Dr. V.A. J. Van Lint Dr. J.L. Russell	1 1
General Dynamics Corp. Grants Lane Fort Worth 1, Tex. ATTN: Mr. E.L. Burkhard	1
General Electric Co. Re-Entry Systems Dept 3198 Chestnut St. Philadelphia 1, Pa ATTN: Mr. J.F. Duncan	1
General Electric Company Power Tube Dept Bldg 269 1 River Rd Schenectady, N.Y ATTN: Mr. David J. Hodges	1
General Electric Co. Radiation Effects Operation, Bldg 14, Electronics Park Syracuse, N.Y. ATTN: Mr. John Sinisgalli	1
General Electric Company Radiation Effects Operations Bldg 14, Electronics Park Syracuse, N.Y ATTN: Mr. L. Dee	1

Address	No. of copies
Georgia Institute of Technology and Engineering Experiment Station, 722 Cherry Street, N.W. Atlanta 13, Ga. ATTN: Dr. R.B. Belser	1
Hughes Aircraft Company Florence and Teale Streets Culver City, Calif. ATTN: Dr. C. Perkins	1
Hughes Aircraft Company Ground Systems Group 1901 W. Malvern Ave. Fullerton, Calif. ATTN: Mr. T.D. Hanscome MS 393/B122	1
International Business Machine Corporation Route 17C Owego, N.Y. 13827 ATTN: Mr. Bohan	1
Lockheed Aircraft Corporation Missile & Space Division 1111 Lockheed Way, Sunnyvale, Calif. ATTN: Mr. H.D. Warshaw, Department 58-11	1
Martin-Marietta Corp. Friendship Rd. Friendship Intl. Airport Baltimore, Md.	1
Martin-Marietta Corporation Middle River Baltimore, Md.	1
Massachusetts Inst. of Technology Lincoln Lab. 244 Wood St. Lexington, Mass. ATTN: Documents Librarian	1
Motorola Semiconductor Projects Div. 5005 East McDowell Rd. Phoenix, Arizona ATTN: Mr. Joseph L. Flood	1

Address	No. of copies
New York University Washington Square, New York, N. Y. 10003 ATTN: Prof. H. P. Kallmann,	1
North American Aviation Corp. Atomics International Div. 21600 Van Owen St. Canoga Park, Calif. ATTN: Dr. A. Saur	1
North American Aviation Corp. Autonetics Div. 9150 Imperial Highway Downey, Calif. ATTN: Mr. T. C. Getten	1
Northrup Vantura 1515 Rancho Conejo Blvd. Newbury Park, Calif. 91320 ATTN: Dr. T. M. Hallman	1
Radio Corporation of America Harrison, N. J. 07029 ATTN: Mr. J. J. Corrona	1
Radio Corporation of America New Holland Pike Lancaster, Pa ATTN: Mr. Herman A. Stern	1
USAF Project RAND, Via AF Liaison Office The RAND Corporation 1700 Main Street Santa Monica, Calif. ATTN: Mr. J. Whitener	1
Raytheon Co., 55 Chapel St., Newton 58, Mass. ATTN: Mr. Francis J. Barry	1
President, Sandia Corporation Sandia Base, Albuquerque, N. Mexico 87115 ATTN: Dr. J. W. Easley, 5300	1

Address	No. of copies
President, Sandia Corporation Sandia Base, Albuquerque, N. Mexico 87115 ATTN: Dr. Carter D. Broyles 5413	1
President, Sandia Corporation Sandia Base, Albuquerque, N. Mexico 87115 ATTN: A.W. Synder, 5313 ATTN: S.C. Rogers 5321	1
Sperry Gyroscope C y. Mail Stop 1A36 Great Neck, N.Y. 11020 ATTN: Mr. J. Rogers	1
Stevens Institute of Technology 501 and 711 Hudson Street Hoboken, N.J. ATTN: Dr. E.J. Henley	1
Sylvania Electric Prod. Inc. Euporium, Pa. 15834 ATTN: Mr. H.C. Pleak	1
Sylvania Electric Products, Inc. Microwave Device Division 1891 East Third St. Williamsport, Pa. ATTN: Mr. John H. O'Neill	1
TRW Space Technology Labs Thompson-Ramo-Woolbridge, Inc. 1 Space Park, Redondo Beach Calif.	1
Tung-Sol Electric, Inc. 200 Bloomfield Ave. Bloomfield, N.J. ATTN: Mr. Max Bareiss	1
Varian Associates 611 Hansen Way Palo Alto, Calif. ATTN: Dr. J. Haimson	1

Address	No. of copies
U.S. Army Electronics Laboratories ATTN: AMSEL-RD-PE ATTN: AMSEL-RD-PF Fort Monmouth, N.J. 07703	 1 1
U.S. Atomic Energy Comission Office of Technical Information Extension P.O. Box 62 Oak Ridge, Tenn.	3
Scientific & Technical Info. Facility ATTN: NASA Rep. (SAK/DL-462) P.O. Box 5700, Bethesda, Md. 20014	 1
Commanding General, USAECOM ATTN: AMSEL-RD-PEM (Dr. I. Bady AMSEL-RD-PEE (Mr. N. Lipetz) AMSEL-RD-PRM (Mr. W.H. Wright) Fort Monmouth, New Jersey 07703	 1 1 1
General Electric Co., Receiving Tube Dept 316 East Ninth St. Owensboro, Ky. ATTN: Mr. Daniel D. Mickey	 1
General Electric Co. 601 California Avenue Palo Alto, Calif. ATTN: Dr. F.B. Fank	 1
Procedyne Associates, Inc. 221 Somerset St. New Brunswick, N.J. ATTN: Dr. Robert Staffin	 1
State of New York Executive Dept Office of Atomic Development P.O. Box 7036 Albany, N.Y. ATTN: Mr. Oliver Townsend	 1

Address	No. of copies
Sperry Microwave Electronics Co. P.O. Box 1828 Clearwater, Florida 33557 ATTN: Dr. Gordon R. Harrison	1

This contract is supervised by the Techniques Branch, Electron Tubes Division, ECD, USAECOM, Ft. Monmouth, N.J. For further technical information contact Frank Palmisano, Project engineer, telephone 201-59-61581.

AD Div. 8 4, 14 11, 17 9

Sperry Microwave Electronics Company, Division of Sperry Rand Corporation, Clearwater, Florida.
STUDY OF PULSED RADIATION EFFECTS ON MICROWAVE FERRITE DUPLEXERS. By R. E. Greenwood and G. R. Harrison. Seventh Quarterly Report - 1 November 1963 to 29 February 1964. 39 pp Inc. Illus.-Graphs. 9 refs. Rpt. No. SJ-222-0041-7

Contract No. DA36-039-SC-85330 Unclassified Report

This report presents the results of the fifth series of radiation environmental experiments conducted during the seventh quarter of the program. Included in the report are a description of the equipment used to perform the experiments, the measurement techniques employed and a complete dosimetry report. Photographs of important phases of the test are given to provide the reader with a better insight into the study. The microwave high power tests, which were initiated during the fourth series of tests, were continued for the fifth series of experiments. Conclusions presented are based upon the data taken thus far, including the fourth and fifth series of tests with high power operation.

UNCLASSIFIED

1. Study of Pulsed Radiation Effects in Ferrite Duplexers
2. Duplexers, C-Band
3. Circulator, ferrite
4. Gyromagnetic coupling ferrite limiter
5. Isolator, ferrite
I. Radiation effects
II. R. E. Greenwood
III. G. R. Harrison
IV. U. S. Army Electronics R&D Laboratory, Ft. Monmouth, N. J.
V. Contr. DA36-039-SC-89113

UNCLASSIFIED

AD Div. 8 4, 14 11, 17 9

Sperry Microwave Electronics Company, Division of Sperry Rand Corporation, Clearwater, Florida.
STUDY OF PULSED RADIATION EFFECTS ON MICROWAVE FERRITE DUPLEXERS. By R. E. Greenwood and G. R. Harrison. Seventh Quarterly Report - 1 November 1963 to 29 February 1964. 39 pp Inc. Illus.-Graphs. 9 refs. Rpt. No. SJ-222-0041-7

Contract No. DA36-039-SC-85330 Unclassified Report

This report presents the results of the fifth series of radiation environmental experiments conducted during the seventh quarter of the program. Included in the report are a description of the equipment used to perform the experiments, the measurement techniques employed and a complete dosimetry report. Photographs of important phases of the test are given to provide the reader with a better insight into the study. The microwave high power tests, which were initiated during the fourth series of tests, were continued for the fifth series of experiments. Conclusions presented are based upon the data taken thus far, including the fourth and fifth series of tests with high power operation.

UNCLASSIFIED

1. Study of Pulsed Radiation Effects in Ferrite Duplexers
2. Duplexers, C-Band
3. Circulator, ferrite
4. Gyromagnetic coupling ferrite limiter
5. Isolator, ferrite
I. Radiation effects
II. R. E. Greenwood
III. G. R. Harrison
IV. U. S. Army Electronics R&D Laboratory, Ft. Monmouth, N. J.
V. Contr. DA36-039-SC-89113

UNCLASSIFIED